This is a PDF file of an article that has undergone enhancements after acceptance, such as the addition of a cover page and metadata, and formatting for readability, but it is not yet the definitive version of record. This version will undergo additional copyediting, typesetting and review before it is published in its final form, but we are providing this version to give early visibility of the article. Please note that, during the production process, errors may be discovered which could affect the content, and all legal disclaimers that apply to the journal pertain.

Application of $BiOCl_nBr_m$ photocatalyst to cytostatic drugs removal from water; mechanism and toxicity assessment

Patrycja Wilczewska[1], Andrea Elisabeth Natasha Ona[2], Aleksandra Bielicka Giełdoń[1], Anna Malankowska[1], Karol Tabaka[1], Jacek Ryl[3], Filip Pniewski[4], Ewa Maria Siedlecka[1*]

[1]Faculty of Chemistry, University of Gdansk, Wita Stwosza 63, 80-308 Gdansk, Poland

[2]Escurla Politécnica Nacional, Departamento de Ingeniería Civil y Ambiental, Centro de Investigación y Control Ambiental, Ladrón de Guevara E11-253, Quito, Ecuador, P.O. Box 17-01-2759.

[3]Faculty of Chemistry, Gdansk University of Technology, Narutowicza 11/12, 80-233 Gdansk, Poland

[4]University of Gdańsk, Institute of Oceanography, Laboratory of Marine Plant Ecophysiology, al. Marszałka Piłsudskiego 46, 81-378 Gdynia, Poland

*Coresponding author:

Ewa Siedlecka e-mail: ewa.siedlecka@ug.edu.pl; phone: +48 58 5325228

Abstract

The photocatalytic activity of series of $BiOCl_nBr_m$ photocatalysts toward degradation and mineralization of the cytostatic drugs 5-fluorouracil (5-FU) and imatinib mesylate (IMA) both singly and in their mixture under simulated solar and visible light irradiation has been investigated. Screening test revealed that among $BiOCl_nBr_m$ photocatalysts synthesized by a solvothermal method, the one with molar 1.3Cl/0.7Br ratio was the most efficient in 5-FU removal under UV-Vis irradiation. The dose 200 mg L^{-1} and 6.3 pH were optimal to effective removal of 5-FU. The BiOCl1.3Br0.7 was successfully used to 5-FU and IMA removal singly and in their mixture under simulated solar and visible light irradiation. Scavenging experiments showed that h$^+$ and $^\bullet O_2^-$ were the major oxidative species participated in both drugs degradation. In presence of IMA, 5-FU removal was significantly depressed. In singly drug solutions and in the mixture of drugs, the presence of inorganic ions such as Cl$^-$, SO_4^{2-}, and NO_3^- significantly hindered 5-FU photocatalytic degradation, and increased the adsorption of IMA onto the photocatalyst surface in dark phase. The HCO_3^- anion, Fe^{3+} and Ag^+ cations accelerated the 5-FU removal, while Ca^{2+} showed no impact on the process. The transformation products of 5-FU and IMA were identified by LC-MS revealing that hydroxylation and oxidation were the

main transformation pathways, under the all studied systems. Some of intermediates were indicated for the first time in heterogeneous photocatalysis. The defluorination of 5-FU by the reaction with photogenerated e$^-$ was also possible. Furthermore, the alga toxicity assay was investigated using *Chlorella vulgaris*. A reduction of toxicity in effluents after photocatalytic degradation of both drugs singly and in their mixture was observed.

Keywords: photocatalysis; 5-FU; IMA; cytostatic drugs; kinetics; degradation mechanism; inorganic ions

1. Introduction

A wide range of pharmaceuticals and personal care products have been detected in groundwater and surface water affected by various wastewater effluents [1]. Major sources of these contaminants are associated with hospitals, households farming (animals, fish) and other industrial-scale agricultural activities. Pharmaceutical compounds are biologically active in trace quantities and conserve their behavior after being discharged into aquatic environments, raising concerns regarding the potential risks to the environment and human health [2]. Due to the hydrophilicity and inherent resistance of many pharmaceuticals to biodegradation, this implies that numerous groups of pharmaceuticals could pass intact through conventional water treatment facilities [1].

An important class of pharmaceuticals are cytostatic drugs, which in many cases characterized the high cytotoxicity, genotoxicity, mutagenicity and teratogenicity. Many anti-cancer or cytostatic drugs occur in wastewater effluents and environmental systems [3,4]. In this group, most commonly used is 5-fluorouracil (5-FU). The existence of 5-FU in the environment is at a concern due to its persistence and similar structure to one of the major components of DNA, uracil. Ecotoxicity assessment of 5-FU showed several effects that depended on its concentration and type of examined organism, but the experimental data concerning the actual concentrations of 5-FU in the environment are still limited [5]. Its presence in rivers, municipal urban and hospital wastewaters at concentration of 280 ng$\cdot$L^{-1}, 5.0-160 ng$\cdot$L^{-1} and 46-1500 ng$\cdot$L^{-1}, respectively, was reported by Booker et al. [7]. The use of imatinib (IMA) as an innovative anticancer drug for chronic myeloid leukemia treatment is continuously rising causing an increase of IMA concentration in the environment. The environmental concentration of IMA has been estimated at a level around 5 ngL^{-1} in France [6],

England [7] and Portugal [8]. Imatinib even at very low concentration can effect on the organisms by interfering with development or damaging DNA [9]. The effects which can 5-FU and IMA induce on environmental are worrying and it is required to find a way of removing them from the wastewater.

It was reported that Advanced Oxidation Processes (AOPs) such as photocatalytic processes can effectively eliminate organic contaminants without producing secondary waste in the environment [10, 11]. Photocatalytic oxidation has been shown to be a promising technique due to its non-toxicity, lack of mass transfer limitation and possible operation at ambient temperature. Heterogeneous photocatalysis offers the possibility of oxidation of organic matter directly through the generation of holes (h^+) or indirectly by the production of hydroxyl radicals ($^\bullet OH$) [12]. For these reasons photocatalysis is considered to be a post-treatment option for the oxidative decomposition of emerging organic contaminants that remain after biological treatment [13]. However, presence of inorganic anions and cations in water is important from the point of view of photocatalytic processes. Ions can act as a radical scavenger and/or a precursor of reactive species, modify pH of solutions or block active sites of photocatalysts surface. Therefore, the evaluation of photocatalytic activity should be also conducted with an addition of inorganic ions. More complex approach is a key parameter to design, implementation and operation AOPs of water treatment processes.

Bismuth oxyhalides (BiOX) semiconductors are the most important bismuth-based photocatalysts. Their unique layered structure with the $[Bi_2O_2]^{2+}$ slabs intersected by double slabs of halogen atoms results them high photocatalytic activity in visible light. $[Bi_2O_2]^{2+}$ blocks and interlayer with halogen ion layers (X) causes favor the self-building of an internal static electric field. This electric field is helpful in the separation and migration of photogenerated carriers e^-/h^+ [14, 15]. On the other hand, the band structure of the material, especially position of conduction band (CB) is very important for its energy exploitation efficiency and photocatalytic properties. Theoretical calculations have shown that the conduction band position of bismuth-based compounds mainly consists of Bi 6p orbitals. Therefore, the increase in the content of bismuth may affect the CB potential [16]. According to our knowledge, there are no reports on the optimal molar ratio of chlorine to bromine bismuth rich oxyhalides used for cytostatic drugs removal from aqueous solution.

In this work, a novel photocatalysts $BiOCl_nBr_m$ synthesized via solvothermal method varying the molar ratio of halogen ions Cl^- to Br^- (x =0.0-2.0) were developed. The correlation between Cl:Br molar ratio and photocatalyst characterization and activity was also analyzed. A synergistic effect between chloride and bromide determined the high photocatalytic activity of

$BiOCl_nBr_m$ in drugs removal under simulated solar and visible-light radiation. Furthermore, this study demonstrates the potential application of $BiOCl_nBr_m$ photocatalysts for the removal of anticancer pharmaceuticals from their mixtures. The influence of photocatalysts dose and pH of solution during the photocatalytic processes were explored. Also, the impact of some inorganic anions and cations on the performance $BiOCl_nBr_m$ photocatalysts for the treatment of pharmaceuticals was evaluated. In this research the mechanisms of degradation of 5-FU and IMA were investigated and discussed in detail, which can be helpful in application of photocatalysis to remove the drugs from water. The formation of intermediate reaction products was investigated by LC-MS. In order to ensure that photocatalytic degradation of cytostatic drugs did not create more toxic intermediate products mixture, the toxicity toward *Chlorella vulgaris* was assessed.

2. Material and methods

2.1 Materials

Bismuth nitrate, Potassium chloride and Glycerol, Acetone, Sodium chloride and Calcium nitrate, Potassium dichromate, Sodium dicarbonate were purchased from StanLab Sp. J. (Lublin, Poland), Potassium bromide were purchased from Alfa Aesar, Ethyl alcohol, chloroform, *tert*-butyl alcohol, 1,5-Diphenylcarbazide, Rhodamine B, Sodium phosphate, Iron (III) nitrate, Sodium sulfate and Sodium nitrate were purchased from POCh S.A. (Gliwice, Poland) and 5-Fluorouracil, Imatinib mesylate, *p*-Benzoquinone, Nitrotetrazolium Blue chloride, Silver nitrate and Acetonitrile were obtained from Sigma-Aldrich (Steinheim, Germany). L - (+) ascorbic acid was obtained from Chempur® (Piekary Śląskie, Poland) and Na_2EDTA dehydrate (certified reference material) was provided from Acros Organics. All reagents were used in analytical grade and without further purification. Works with cytostatic drugs were carried out following the recommendation of the European Commission: "Preventing occupational exposure to cytotoxic and other hazardous drugs [17]. More details about prevention were presented in Supplementary materials

2.2 Synthesis of series of $BiOCl_nBr_m$

Stoichiometric amounts of KCl and KBr were dissolved in 20 mL glycerol to obtain the solution A. $Bi(NO_3)_3 \cdot 5H_2O$ (2 mmol) was dissolved in 20 mL glycerol to obtain the solution B. Then, the solution A was added by drops to the solution B while strong magnetic stirring. The suspension was transferred into Teflon-lined stainless steel autoclaves (50 mL) and kept at 160°C for 16 h. After the reaction was completed, the formed complex precursor precipitate

was obtained by centrifugation and washed with ethanol for three times. After that, resulting complex precursor was dried at 80 °C under air atmosphere. $BiOCl_nBr_m$ solid solutions were obtained by a simple hydrolysis in water, in which 0.3 g of the complex precursor molecules with 100 mL of deionized water was mixed. Finally, the compounds were rinsed with deionized water and dried at 80 °C [18]. A variety of Cl/Br mole ratio (from 0 to 2) were used to optimize the content of the individual halogen in the nanomaterial. Obtained photocatalysts were listed in Table 1.

2.3 Characterization of prepared photocatalysts

The crystalline structures and compositions of $BiOCl_nBr_m$ samples were made an X-ray diffraction (XRD) analysis with PANalytical X'Pert Plus diffractometer with focusing primary monochromator CuKα (λ = 1.54 Å) radiation. In order to identify the morphologies, sizes and structure of the synthesized photocatalyst, scanning electron microscopy (*JEOL JSM-7610F* FEG-*SEM)* was performed. The optical properties were analyzed using UV–Vis diffuse reflectance spectra (DRS) which were obtained by 2600 UV-VIS SPECTROPHOTOMETR Shimadzu and $BaSO_4$ was used as a reference. The photoluminescence spectrum (PL) was obtained by Perkin Elmer limited LS50B spectrophotometer in the range of 300–700 nm. Excitation wavelength was 315 nm. The Brunauer–Emmett–Teller (BET) surface area and pore size distribution analyzes were measured by nitrogen adsorption–desorption test (Micromeritics Gemini V Surface Area and Pore Size analyzer) with automated gas sorption system at 77 K. X-ray photoelectron spectroscopy (XPS) with ThermoFisher Scientific Escalab 250Xi was used to determine the composition of the surface of the $BiOCl_nBr_m$.

2.4 Photocatalytic activity measurements

2.4.1   Screening test of activity under UV-Vis irradiation

To select photocatalyst with the highest activity, a 150 W Heraeus medium pressure mercury lamp with cooling system was used as UV-Vis source in the screening test of 5-FU photocatalytic degradation in the presence of series of $BiOCl_nB_{rm}$. The drug solution of 15 mg L^{-1} with 0.2 g L^{-1} photocatalyst was illuminated for 120 min in multi-station reactor. The distance between each 15 ml reactor and light source was 3 cm. Before irradiation starts, the suspension was magnetically stirred in the dark for 30 min to establish an equilibrium of adsorption-desorption between the photocatalyst and the organic compound. Then, during

photocatalytic process with continuously stirring, one milliliter of the aqueous suspension was taken in each certain interval of time and filtered through 0.22 μm syringe filter to remove solid particles. Each test of photocatalytic activity was repeated twice. The concentration of cytostatic drugs in each sample was analyzed in triplicate by HPLC technique [19]. 5-FU was detected using acetonitrile/water 2:98 (v/v) as the mobile phase, an elution time was 4.9 min and a detection wavelength was 266 nm. The concentration of IMA was analyzed using acetonitrile/0.1% formic acid water solution 10:90 (v/v) as the mobile phase, retention time was 5.1 min and detection wavelength w302 nm. A Phenomenex C18 column (150 mm x 4.6 nm, 2.6 μm) was used for chromatographic analysis of both drugs.

2.4.2 Drugs degradation under artificial solar light and visible light

The activity of selected photocatalyst and optimization of working parameters were tested toward 5-FU, IMA and their mixture degradation in Suntest CPS+ solar simulator (Atlas Matrial Testing Technology LLC) equipped with cooling and stirring systems, with a 1700W Xenon lamp as the light source and an intensity of 430 W/m^2 (the average value e.g. Seville in Spain in summer in 2010) as artificial sunlight and with 420 nm cut off filter as visible light source. Suntest CPS+ is a simulator of sunlight recommended by OECD. Before 180 min of illumination, suspension of photocatalyst was kept in the dark for 30 min. Initial concentrations of cytostatic drugs and photocatalyst were 15 mg L^{-1} and 0.2 g L^{-1}, respectively. The temperature of experiments was maintained at 25°C, and volume of reactor was 50 mL. The distance between reactor and light source was 15 cm. As it was described in section 2.4.1. the samples after filtration were analyzed by HPLC. The mechanisms of degradation of 5-FU and IMA in the presence of BiOCl1.3Br0.7 under sunlight radiation was proposed based on information provided by the *in situ* experiments with Na$_2$EDTA, *para*-benzoquinone/ascorbic acid, chloroform and *tert*-butyl alcohol in amount of 10 mM, as a scavengers of holes, superoxide anion radicals, electrons and hydroxyl radicals, respectively. Due to reactivity of p*ara*-benzoquinone with IMA (which has been found in the experiments), the ascorbic acid as an effectively scavenger of $^\bullet O_2^-$ in the presence of IMA was used. The remaining experimental conditions were identical as in drugs degradation experiments under artificial solar and visible light. Amount of generated $^\bullet OH$ and $^\bullet O_2^-$ during irradiation was evaluated through terephthalic acid (TA) and nitroblue tetrazolium chloride (NBT) tests, respectively [20, 21]. The absorbance of NBT was measured at 259 nm. Effect of photocatalyst dosage (0.2 – 1 g L^{-1}) and pH (3-10.5) on photocatalytic degradation of 5-FU was examined. Research also included determination the

effect of anions (Cl^-, SO_4^{2-}, HCO_3^-, NO_3^-) and cations (Ca^{2+}, Fe^{3+}, Ag^+) on cytostatic drugs and their mixture decomposition. The concentration of the respective ions added to drug solution or their mixture was 3 mM [22]. Each test of photocatalytic activity was repeated twice. The drugs mineralization was analyzed using the total organic carbon (TOC) and total nitrogen (TN) analyzer (Total Organic Carbon analyzer, Total Nitrogen Measuring UNIT Shimadzu). The final concentration of cytostatic drugs was analyzed in triplicate in each sample by HPLC-UV. Photocatalytic decomposition pathways of 5-FU and IMA were proposed based on organic products detected by LC-MS [19]. The analytical methods were described in details in our previous study [23].

The degradation products were identified with the use of an Agilent 1200 Series LC system (Agilent Technologies, Inc., Santa Clara, USA) coupled to an HCT Ultra ion trap mass spectrometer (Brucker Daltonics, Bremen, Germany). The MS analysis was conducted by using positive and negative mode electrospray ionization (ESI) under the following conditions: capillary 4 kV, nitrogen as the drying gas with flow rate 10 L min^{-1}, drying temperature 350 °C, nebulizer 30 psi, and the maximum accumulation time of 200 ms. All ions were monitored in a full scan mode, and then the chosen ions were monitored in a selected ion monitoring (SIM) mode.

2.5 Algal growth inhibition test

The algal growth inhibition tests were carried out using green alga strain *Chlorella vulgaris* Beijernick BA-02 isolated from the coastal waters of the southern Baltic Sea and maintained as a unialgal culture in the Culture Collection of Baltic Algae (CCBA) at the Gdansk University [24]. The toxicities of 5-FU (0-50 mg L^{-1}), IMA (0-50 mg L^{-1}), their combination (5-FU+IMA; 15+15 mg L^{-1}) as well as photocatalytic oxidized mixtures of each of the compound (5-FU - 15 mg L^{-1}, IMA - 15 mg L^{-1}, 5-FU+IMA - 15+15 mg L^{-1}) were tested by means of a graduated dilution. In brief, tests were carried out in glass Erlenmeyer flasks with the final volume culture of 10 mL [25]. Before each test *C. vulgaris* cells were acclimatized to the culturing conditions until cells reached the exponential growth phase. Subsequently they were exposed to a serious of graded concentrations of the tested drugs and their oxidation mixtures. Algal cultures were kept under constant light and temperature conditions, i.e. at 100 μmol m^{-2} s^{-1} provided in a 16:8 light:dark cycle and temperature of 18±1 °C. Each test was carried out in triplicate covering a range of 11 concentrations arranged according to ISO standards [26]. In each test the initial cell density was 5 x 10^4 cells mL^{-1}. Cultures were exposed to the experimental conditions for 96h [27] during which they were vigorously shaken every 12h. After this time a cell density of each

culture was estimated by counting cells in hemocytometer with Bürker grid. Subsequently, the inhibition growth rate and EC_{50} values were calculated (ISO 10253:2006 guideline). Differences between calculated means were tested using analysis of variance (ANOVA) and Post-hoc Tukey HSD test.

3. Results and discussion

3.1 Photocatalysts characterization

3.1.1 XRD analysis

X-ray powder diffraction was used to determine the crystal phase of prepared photocatalysts. Figure 1 shows XRD patterns for $BiOCl_nBr_m$ samples obtained via solvothermal method.
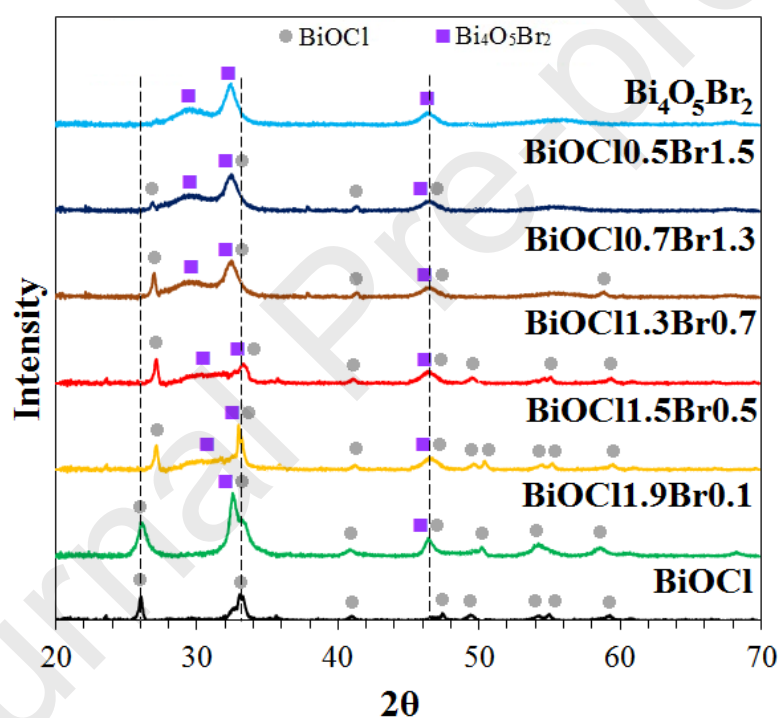
Figure 1. XRD patterns for $BiOCl_nBr_m$ samples prepared via solvothermal methods.

The XRD patters revealed the existence of the pure BiOCl (ICDD 01-085-0861) and pure $Bi_4O_5Br_2$ (ICDD 00-037-0699) for molar ratio Cl/Br 2/0 and 0/2, respectively. Diffraction peaks 33.1° and 47.0° of BiOCl1.9Br0.1 were wider and shifted compared in BiOCl which suggested that Br⁻ was introduced into crystal lattice of BiOCl and created $BiOCl_nBr_m$ phase. Furthermore, diffraction peak 26° corresponding to plane (101) was shifted to smaller angle which indicated that $BiOCl_nBr_m$ was solid solution [28, 29]. With increasing content of Br⁻ ions, $Bi_4O_5Br_2$ phase

was created as a coexistence of $BiOCl_nBr_m$ phase, and the peaks intensity of $BiOCl_nBr_m$ phase was decreased. All samples displayed broad diffraction signals revealing the formation of small particle size [30]. Table 1 summarized the results of the XRD measurements.

Table 1. Summarized the results of synthesized samples characterization.

Label	Molar Cl/Br ratio	Crystalline phase	Eg [eV]	S_{BET} [m^2g^{-1}]	Total pore volume [cm^3g^{-1}]	XPS analysis Elements			
						Bi	O	Cl	Br
BiOCl	2/0	BiOCl	3.34	90.7	0.043	31.59	44.06	24.35	0
BiOCl1.9Br0.1	1.9/0.1	$BiOCl_nB_{rm}$	3.1	-	-	-	-	-	-
BiOCl1.5Br0.5	1.5/0.5	$BiOCl_nB_{rm}/Bi_4O_5Br_2$	3.08	-	-	-	-	-	-
BiOCl1.3Br0.7	**1.3/0.7**	**$BiOCl_nB_{rm}/Bi_4O_5Br_2$**	**2.90**	**53.9**	**0.027**	**31.94**	**49.22**	**13.08**	**5.76**
BiOCl0.7Br1.3	0.7/1.3	$BiOCl_nB_{rm}/Bi_4O_5Br_2$	2.76	-	-	-	-	-	-
BiOCl0.5Br1.5	0.5/1.5	$BiOCl_nB_{rm}/Bi_4O_5Br_2$	2.78	-	-	-	-	-	-
$Bi_4O_5Br_2$	0/2	$Bi_4O_5Br_2$	2.86	47.9	0.024	37.16	47.39	0	15.45

"-" not measured

3.1.2 SEM analysis

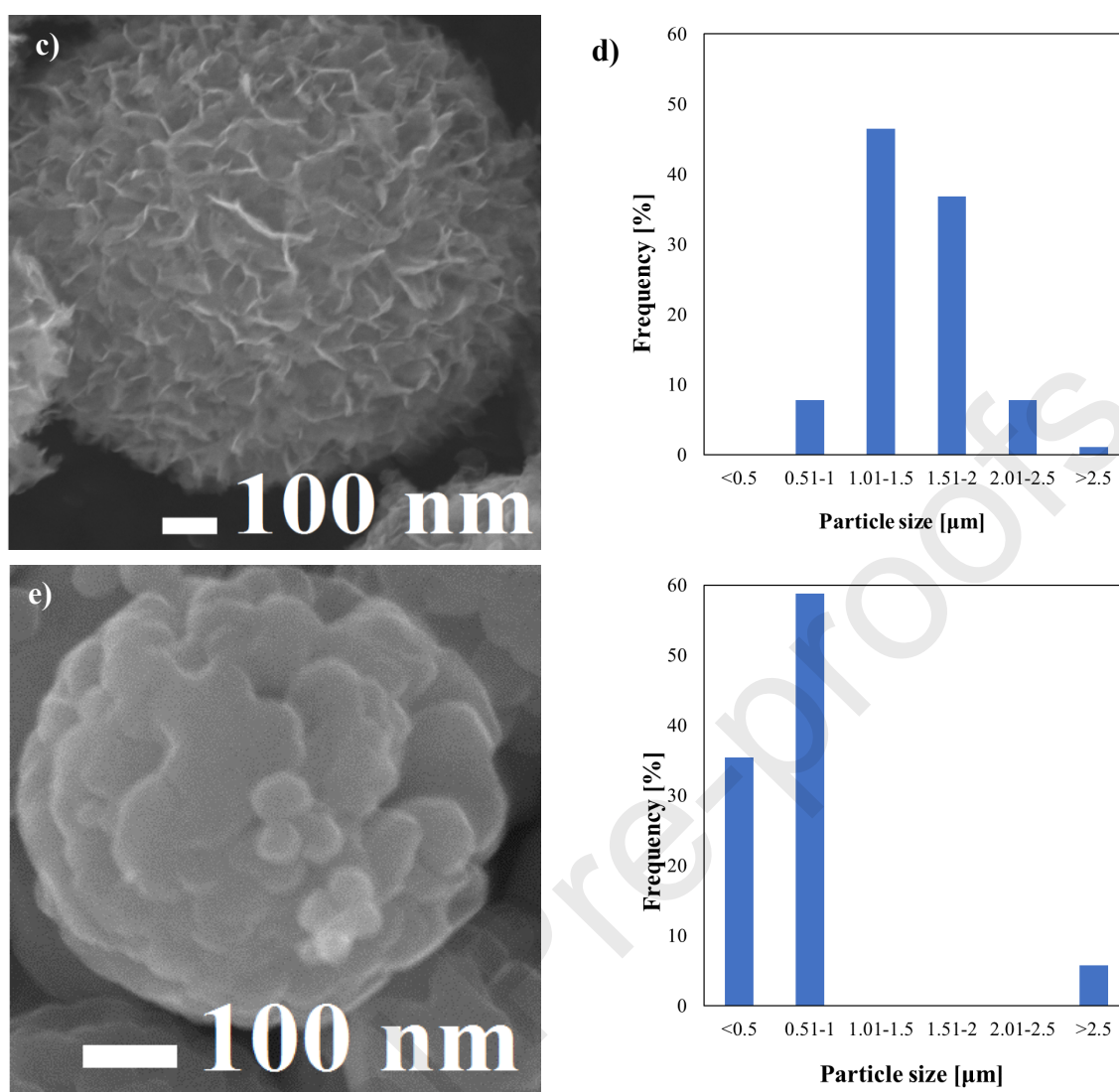The surface morphology of the prepared samples was examined by scanning electron microscopy.
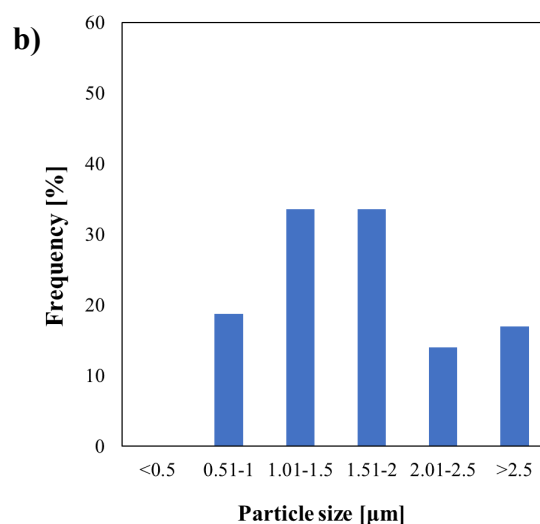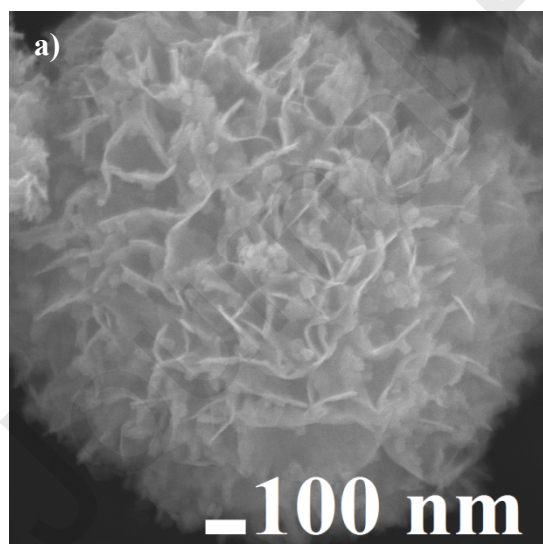
Figure 2. SEM images and particle size distribution graph of a,b) BiOCl, c,d) BiOCl1.3Br0.7 and e,f). $Bi_4O_5Br_2$

Figure 2 showed that prepared BiOCl particles were comprised of many 3D flower-like hierarchical structures looked like in previous reports [23, 31]. These structures were built from several dozen of radially grown very smooth nanosheets with a thickness of about 8-12 nm. In contrast with BiOCl, BiOCl1.3Br0.7 exhibited a relative loose structure. This fact indicated, that presence of Br atoms influenced on the particles size and morphology of the flower-like microarchitectures of photocatalysts. The sample with pure $Bi_4O_5Br_2$ phase was much finer with almost not distinguished nanoplates. Particles size distribution was shown in Figure 2bdf). Introduction bromine atoms to BiOCl was resulted in an increase of the fraction with smaller particles size in BiOCl1.3Br0.7. BiOCl1.3Br0.7 was morphologically more similar to BiOCl than $Bi_4O_5Br_2$.

In further study BiOCl and $Bi_4O_5Br_2$ were used as a reference compounds due to they were the main crystal forms obtained in glycerol for samples with single halogen

3.1.3 BET analysis

Brunauer-Emmett-Teller specific surface area and total pore volume of the $BiOCl_nBr_m$ were investigated by nitrogen adsorption-desorption isotherms and listed in Table 1. It was clearly shown that the BET specific surface area was higher for flowerlike microspheres BiOCl. Compared with the pure samples, BiOCl1.3Br0.7 had similar values of S_{BET} and total pore volume to $Bi_4O_5Br_2$. Furthermore, photocatalysts prepared in glycerol possessed remarkable higher BET specific surface area than reported BiOClxBry solid solution [23, 28, 29, 30, 31].

Generally, the higher BET surface area may lead to the higher photocatalytic activity, however, although the S_{BET} and total pore volume of BiOCl were more developed, its activity was lower than BiOCl1.3Br0.7. Therefore, it is reasonable to conclude that these parameters were not decisive factor influencing the photocatalytic properties in the studied system.

It is worth pointing out that the BET surface of pure BiOCl solvothermally prepared in glycerol was relatively high. Surface of BiOCl fabricated in glycol by Gao et al. [32] was 4.4 times lower (20.6 m^2 g^{-1}) than that obtained in our study.

3.1.4 XPS analysis

In order to confirm the chemical composition and surface chemical states of BiOCl, BiOCl1.3Br0.7 and $Bi_4O_5Br_2$, XPS analysis was conducted and shown in Figure 3. Obtained results from survey spectra suggested that the samples contained the elements of Bi, O, Cl and Br and a trace amount of adventitious carbon without existence of other impurity elements. A high resolution spectra of Bi 4f, Cl 2p and Br 3d were shown in Fig. 3b-d. The obtained binding energies found in Bi4f spectra corresponded to Bi $4f_{7/2}$ and Bi $4f_{5/2}$ and they could be assigned to Bi^{3+} in bismuth oxyhalides [14, 33, 34]. The characteristic peaks of Cl 2p were shown in Fig. 3d. The Cl 2p spectra (Fig. 3d) of BiOCl and BiOCl1.3Br0.7 could be ascribed to Cl $2p_{3/2}$ and Cl $2p_{1/2}$ which were related to Cl^- present in the layered structure of selected photocatalysts. Figure 3c displayed the XPS spectra of Br 3d. The spectra consisted of two signals at energy bindings which could be fitted to Br $3d_{3/2}$ and Br $3d_{5/2}$ characteristic for Br^- in these types of materials [14, 31, 34]. The high resolution spectrum of Bi 4f of BiOCl1.3Br0.7 was more similar to BiOCl than $Bi_4O_5Br_2$ which could be assumed based on the molar ratio of Cl and Br. Signals of Bi $4f_{7/2}$ and Bi $4f_{5/2}$ in $Bi_4O_5Br_2$ and BiOCl1.3Br0.7 spectra were shifted toward higher energies because of higher electronegativity bromine than chlorine. Additionally, peaks

of Cl 2p and Br 3d were also shifted compared to pure BiOCl and $Bi_4O_5Br_2$ spectra, because of second halogen in crystal lattice of BiOCl1.3Br0.7.
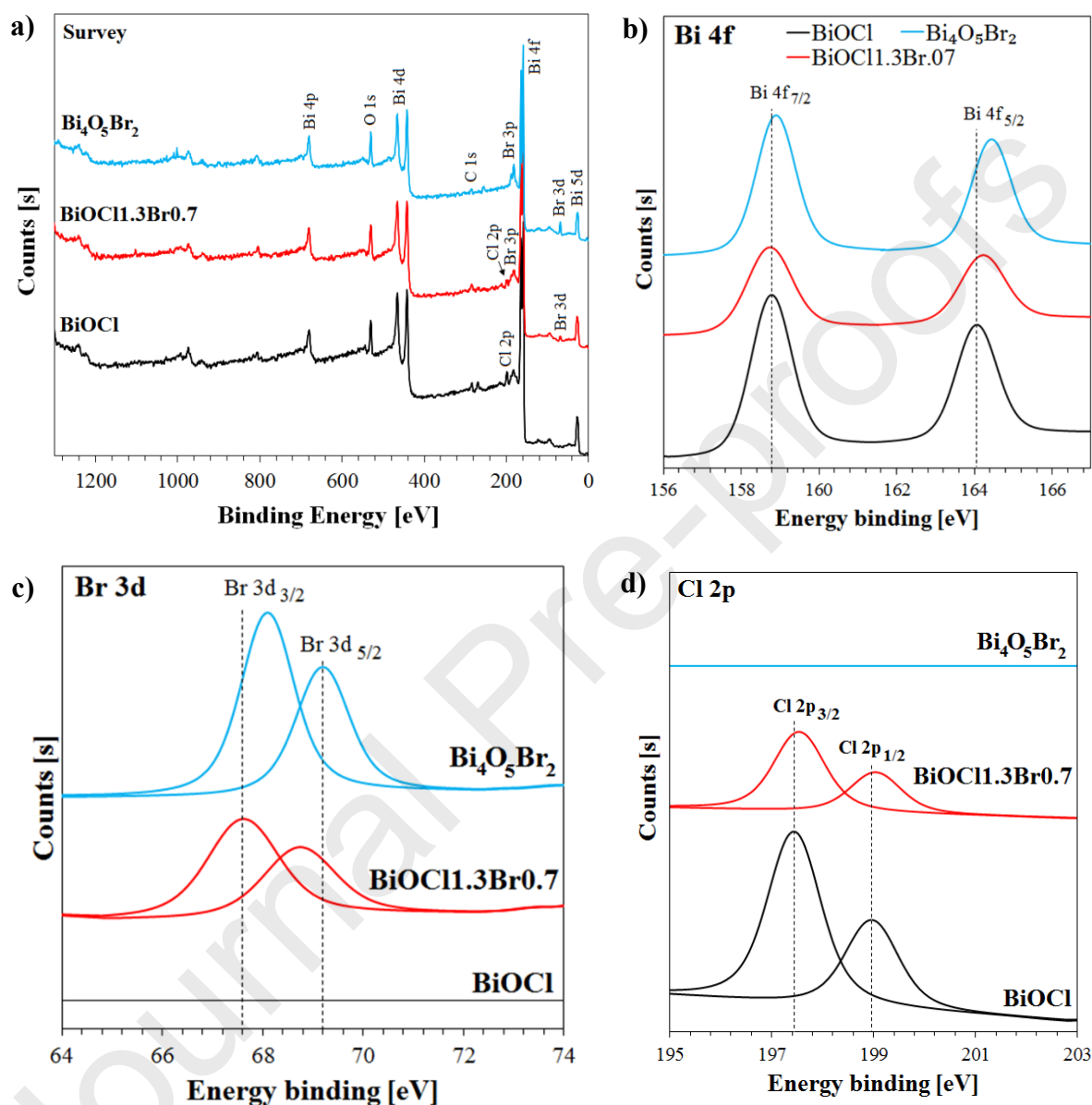

Figure 3. XPS spectra a) the survey, b) Bi 4f, c) Br 3d, d) Cl 2p, of selected photocatalysts BiOCl, BiOCl1.3Br0.7 and $Bi_4O_5Br_2$.

3.1.3 UV-Vis/DRS

The photocatalytic activity of a semiconductor is precisely related to its energy band structure feature. Figure 4a showed the UV–vis diffuse reflection spectra of the synthesized $BiOCl_nBr_m$ in the wavelength range of 250–750 nm.
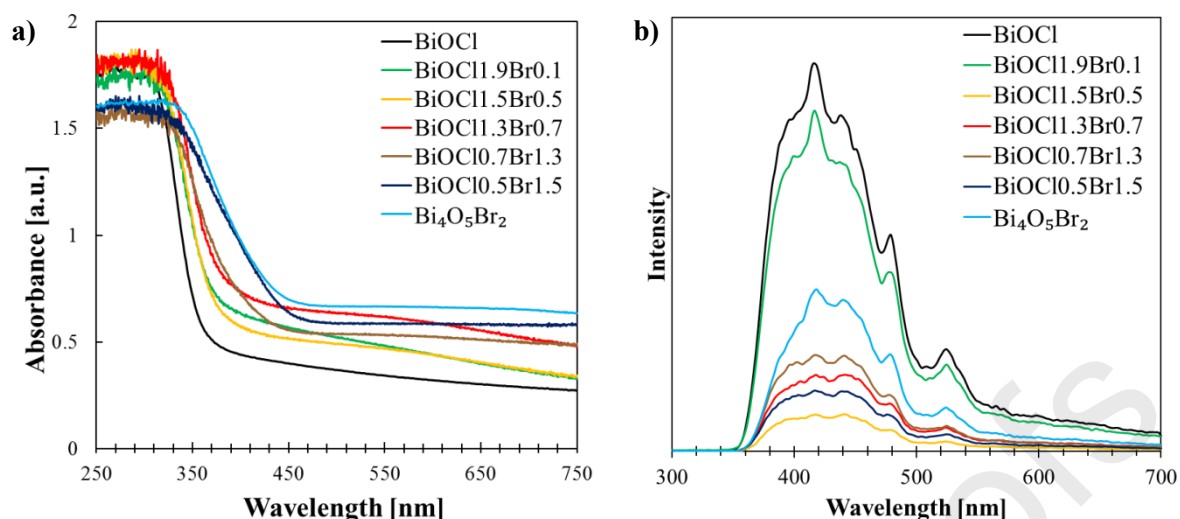
Figure 4. a) U-vis diffuse reflectance spectra of $BiOCl_nBr_m/Bi_4O_5Br_2$ samples and b) Photoluminescence spectra of prepared $BiOCl_nBr_m/Bi_4O_5Br_2$ photocatalysts.

The absorption band-edges of the $BiOCl_nBr_m$ materials were shifted towards the blue waves with the increase of Br-to-Cl molar ratio. The observed blue shift is a positive phenomenon because causes more effectively excited and generated h^+/e^- pairs by visible light which can promote photocatalytic reaction in this light spectrum. $Bi_4O_5Br_2$. was the photocatalyst with the highest visible light adsorption capacity. There was no noticeable relationship between the ratio Br-to-Cl and absorption of light in the wavelength range longer than 420 nm. There was no noticeable relationship between the Br to Cl ratio and light absorption at the wavelengths range greater than 420 nm.

The shape of light absorption curves of photocatalysts with molar ratio Cl:Br 1.9:0.1 and 1.5:0.5 were similar to BiOCl. The difference was the blue shift of spectrum due to presence to Br in crystal lattice. The same relations was observed for semiconductors with more bromine atoms than chlorine atoms in crystal lattice. Addition of chlorine caused redshift. Energy band gap (Eg) values obtained from UV-vis/DRS spectra according to Kubelka-Munk transformation were shown in Table 1. Eg was determined in the range 3.34 - 2.74 eV and it was in accordance with previously reports [33, 34]. The results suggest that the band gap of $BiOCl_nBr_m$ can be well-tuned by rational changing the molar ratios of Cl-to-Br atoms.

3.1.4   Photoluminescence analysis

To investigate the photogenerated charge carriers separation and recombination efficiency during the photodegradation in the presence of $BiOCl_nBr_m$ photoluminescence spectra were measured and shown in Figure 4b. The spectrum of BiOCl possessed the highest intensity due to fast recombination of e^-/h^+, which was one of drawback of this group of photocatalysts [35]. The introduction of a small amount of bromine to BiOCl resulted in the intensity of photoluminescence spectrum decrease as the effect of slower recombination of photogenerated charge pairs. Based on the PL spectra intensity of four samples: BiOCl1.5Br0.5, BiOCl1.3Br0.7, BiOCl0.7Br1.3, BiOCl0.5Br1.5 (Fig 4b), the increase of Br atoms in studied materials accelerated the separation of photogenerated charge carried e^-/h^+.

To sum up, BiOCl1.3Br0.7 showed the morphology and surface properties of BiOCl (XPS, SEM) and $Bi_4O_5Br_2$ (XRD, BET, PL, UV-vis/DRS) and the combination of these phases can effect in remarkable improvement of photocatalytic performance.

3.2 Photocatalytic activity series of $BiOCl_nBr_m$ in 5-FU removal

3.2.1. Screening test

The photocatalytic activity of series of $BiOCl_nBr_m$ in 5-FU degradation was studied at constant initial pH without further adjustment under UV-Vis light (medium pressure Hg lamp) irradiation. In the blank trials, after 180 min of UV-Vis light irradiation the photolysis of 5-FU was negligible. To study the surface adsorption role in photocatalytic drug degradation, dark adsorption experiments for 180 min were conducted to test the 5-FU removal in the absence of light. The adsorption of 5-FU varied from 0 to 7% indicated that adsorption in dark phase was also insignificant (Table 2). The lack of adsorption was not correlated with the variation in surface area and the pore volume of samples described in section 3.1.3. These data were consistent with the properties of 5-FU (low value of log K_{ow}), and suggested that adsorption of this drug does not play a significant role in its removal. The results of screening test over series of prepared photocatalysts were shown in Figure 5.
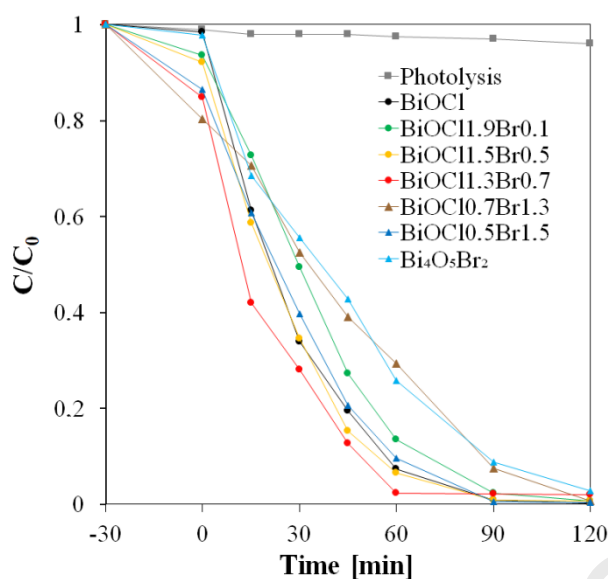
Figure 5. Degradation of 5-FU in presence of $BiOCl_nBr_m$ under UV-vis irradiation.

The reaction kinetics of the 5-FU photodegradation was well fitted to pseudo-first-order equation, and the quantitatively calculated k_{app} was shown in Table 2.

Table 2. The removal of 5-FU in dark phase and the rate constant k_{app} of 5-FU degradation in light phase under UV-Vis light, simulated sunlight (SunTest) and visible light in the presence of series of photocatalysts $BiOCl_nBr_m$.

Photo-catalyst	adsorption of 5-FU* [%]	UV-Vis light Medium pressure Hg lamp (max 366 nm)		Simulated solar light Suntest Xe lamp (λ>290 nm)		Visible light Suntest Xe lamp (λ>420 nm)	
		k_{app} [min^{-1}]	R^2	k_{app} [min^{-1}]	R^2	k_{app} [min^{-1}]	R^2
BiOCl	0	0.046	0.991	0.003	0.992	inactive	inactive
BiOCl1.9Br0.1	2	0.046	0.991	-	-	-	-
BiOCl1.5Br0.5	3	0.050	0.992	-	-	-	-
BiOCl1.3Br0.7	**7**	**0.061**	**0.998**	**0.050**	**0.999**	**0.020**	**0.993**
BiOCl0.7Br1.3	5	0.044	0.998	-	-	-	-
BiOCl0.5Br1.5	3	0.041	0.997	-	-	-	-
$Bi_4O_5Br_2$	3	0.046	0.991	0.031	0.993	0.007	0.992

*Adsorption in dark phase after 180 min; "-" not measured.

The studied BiOCl1.3Br0.7 photocatalyst displayed both the best efficiency of cytostatic drug degradation and the highest rate constant.

Our previous studies have shown that the removal rate of 5-FU under UV-vis light in the presence of $BiOCl_{0.5}Br_{0.5}$ solid solution k_{app} was 0.051 min^{-1} [23]. This value was close to the value of k_{app} calculated for showed in this work BiOCl1.5Br0.5 sample, and lower than the value of k_{app} obtained for BiOCl1.3Br0.7 (0.061 min^{-1}). This fact indicated, that $BiOCl_mBr_n/Bi_4O_5Br_2$ composition prepared in this study more preferably influenced to 5-FU oxidation in contrast to previously prepared $BiOCl_{0.5}Br_{0.5}$ solid solution. Moreover illumination of $BiOCl_mBr_n/Bi_4O_5Br_2$ composition caused quicker drug removal than pure BiOCl or $Bi_4O_5Br_2$ samples [31]. The k_{app} value obtained for 5-FU decomposition in the presence of BiOCl1.3Br0.7 was also higher than that reported by other research group for 5-FU reaction with •OH radicals under Degussa P25 illuminated by UV light [36].

Due to the highest photocatalytic activity toward 5-FU the sample BiOCl1.3Br0.7 was selected to further experiments.

3.3 Photocatalytic activity of BiOCl1.3Br0.7 in drugs removal

3.3.1 Optimization of the 5-FU degradation over BiOCl1.3Br0.7 under simulated sun light

The effect of drug removal during photocatalysis closely depends on working conditions. Due to this fact, the optimal photocatalyst dose and pH of drug solution under simulated sun light irradiation (Suntest) were studied. Sunlight was used to photocatalyst activation, because it is an source of energy for free. The dose of photocatalyst was varied from 100 mg L^{-1} to 1000 mg L^{-1}, keeping other parameters constant (Fig. 6a).
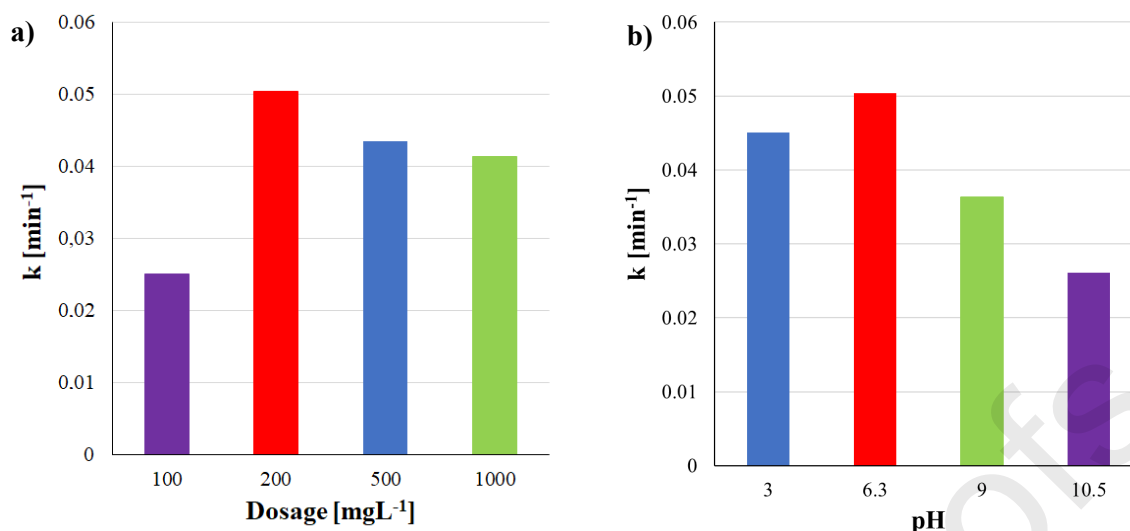
Figure 6. The effect of initial a) dosage of photocatalyst and b) pH solution on degradation of 5-FU under simulated sunlight irradiation.

Increasing dose from 100 mgL^{-1} to 200 mgL^{-1} the rate of 5-FU oxidation was elevated almost twice times. Next, the rate degradation of 5-FU was slightly decreased with further increasing dose of BiOCl1.3Br0.7. Higher dose than 200 mg L^{-1} was unprofitable in process, due to blocking of light by the excess of BiOCl1.3Br0.7 particles. Therefore 200 mgL^{-1} of BiOCl1.3Br0.7 was used for further experiments.

The pH of the aqueous solution is one of the important environmental parameters significantly influences the interaction between semiconductor and micropollutants in water. In Fig. 6b the effect of pH on 5-FU decomposition was shown. The pH$_{zpc}$ of BiOCl1.3Br0.7 was estimated as 6.35, therefore the surface of photocatalyst was positively charged in acidic solutions and negatively charged in alkaline solutions. The highest rate of 5-FU degradation was found for pH of 6.3, while more acidic and alkaline conditions slowed down the oxidation process. Under acidic conditions the inhibition of 5-FU degradation was insignificant, due to undissociated 5-FU form was not interacted with the positively charged surface of photocatalyst [37]. The alkaline pH value caused significant retardment of drug oxidation due to the electrostatic repulsion between negatively charged surface of BiOCl1.3Br0.7 and negatively charged form of 5-FU (pKa$_1$ and pKa$_2$ of 5-FU is 7.53 and 9.01, respectively. Other researcher groups also found that under the alkaline conditions (pH 10) the drug decomposition rate was lower than under neutral conditions [36, 38]. These results are promising from a practical point of view, because the actual pH values of waterbodies are close to neutral value. The pH values of effluents were reported as 7.2-7.7; 5-9 and 7.6±0.4, from the Maria Middelares Hospital WWTP

[39], Aarhus University Hospital WWTP [40] and Hospitals of Babol University of Medical Sciences WWTP [41], respectively.

3.3.2. *The effect of type of light*

The next step of investigations was evaluated the photocatalytic activity of BiOCl1.3Br0.7 sample of photocatalyst in 5-FU degradation under simulated sunlight as an energy for free (λ>290 nm, Xe lamp, Suntest). Due to the fact, that visible light accounts for 45% of solar spectrum, it is significant to develop visible light-driven photocatalysts. Therefore, the activity of prepared photocatalyst under visible light irradiation (λ>420 nm, Xe lamp) was also tested.

As shown in Table 2, BiOCl1.3Br0.7 sample was the most effective in 5-FU degradation under sunlight and visible light irradiation. In contrast BiOCl sample characterized the lowest activity under simulated solar light and it was inactive in low energy visible light illumination. It was the result of relatively high value of energy band gap (Eg) of BiOCl. Under simulated sunlight radiation, the k_{app} calculated for BiOCl1.3Br0.7 was 15 times and 1.5 times higher than that obtained for BiOCl and $Bi_4O_5Br_2$, respectively. Under the visible light the activity of BiOCl1.3Br0.7 in 5-FU degradation (k_{app}) was 2.5 times higher than the activity found for $Bi_4O_5Br_2$. The results suggested the enhancement of photocatalytic activity especially under visible light, by coexistence of $BiOCl_nBr_m$ solid solution and $Bi_4O_5Br_2$ pure phase in prepared materials (Table 1).

3.3.3 Photogenerated entities under simulated solar and visible light

The entities photogenerated in the presence of BiOCl1.3Br0.7 under simulated sunlight and visible light irradiation were studied. The production of the hydroxyl radicals ($^\bullet$OH) was estimated by the oxidation reaction of terephthalic acid (TA). The results revealed that during irradiation $^\bullet$OH radicals were not produced by prepared photocatalysts, regardless of the type of light used. It is according with the results of other research groups [19, 42], which also suggested that •OH radicals were not generated over $Bi_4O_5Br_2$ and BiOCl irradiation. Furthermore, nitroblue tetrazolium chloride (NBT) to determine the amount of superoxide radicals ($^\bullet O_2^-$) produced during photocatalytic reaction in the presence of prepared photocatalysts was used. As shown in Figure 7 after 60 min of illumination of solar light, quantity of $^\bullet O_2^-$ in system with BiOCl and $Bi_4O_5Br_2$ reached plateau in contrast to BiOCl1.3Br0.7. Constantly increasing the amount of photogenerated superoxide radicals using BiOCl1.3Br0.7 suggested the good separation of electrons and holes and it can positively effect on its photocatalytic activity. Introduction Br^- to the crystal lattice of BiOCl improved the

separation of photogenerated electron and holes and enabled generation of $^\bullet O_2^-$ by the electrons. Furthermore, presence of additionally phase $Bi_4O_5Br_2$ provided a large number of additional active sites capable of forming superoxide anion radicals which were observed in NBT experiment.
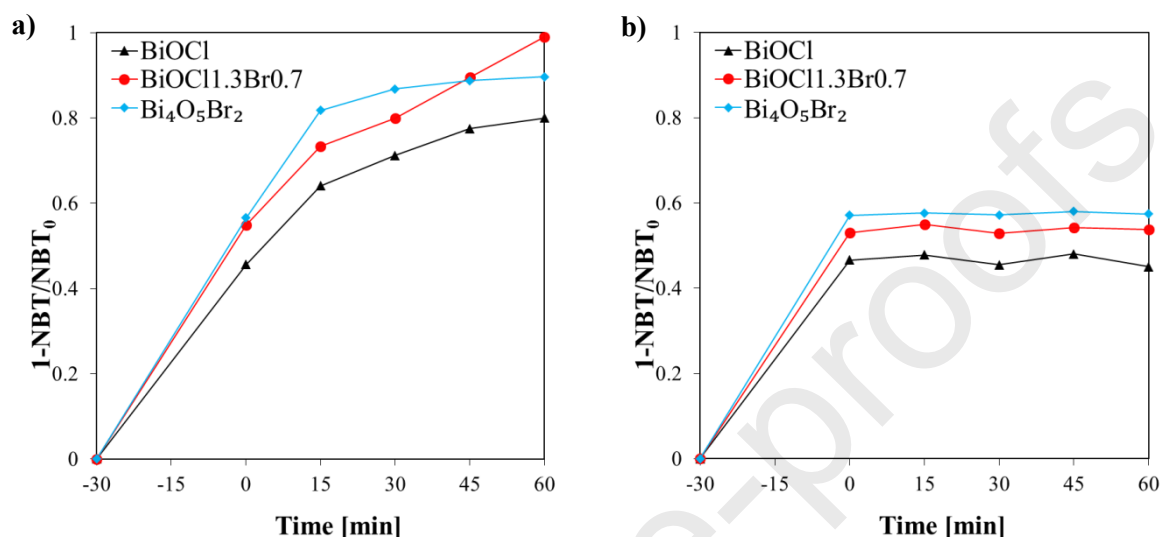

Figure 7. $^\bullet O_2^-$ generation in presence of selected photocatalysts under simulated solar A) and visible B) light irradiation based on the reaction $^\bullet O_2^-$ with the nitroblue tetrazolium chloride (NBT)

Under visible light $^\bullet O_2^-$ radicals were not produced, suggested that holes could be the main oxidants generated under this type of light.

3.3.4. Investigation of the mechanism of 5-FU and IMA decomposition in single drug solution

The mechanism of 5-FU and IMA decomposition under simulated solar and visible light was studied. In absence of photocatalyst 5-FU and IMA were photolytically resistant under both type of light irradiation.

5-FU and IMA were successfully decomposed in the photocatalysis process, however simulated solar light was more efficient than visible light. The decomposition rate of 5-FU and IMA was respectively 2.1 and 2.9 times higher in sunlight than k_{app} in visible light (Figure 8, 9). The complete removal of 5-FU and IMA from solution was achieved in 90 and 60 minutes under solar light, while it took 180 and 120 min under visible light irradiation.

To investigate the role of photogenerated entities in the degradation of cytostatic drugs a number experiments with the appropriate scavengers were conducted (Figure 8, 9).
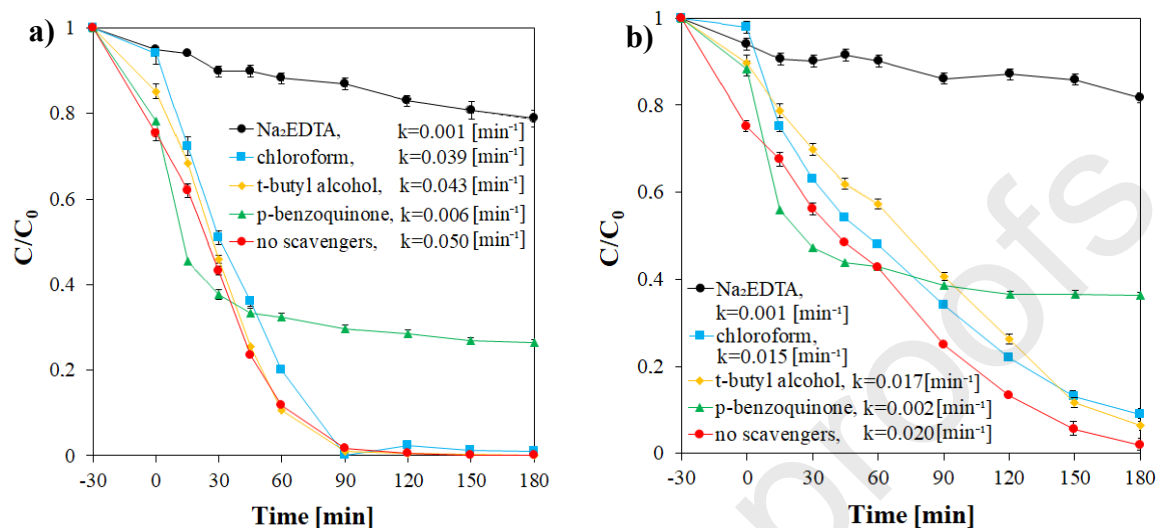

Figure 8. Degradation of 5-FU with and without scavengers under a) sunlight and b) visible light in the presence of BiOCl1.3Br0.7
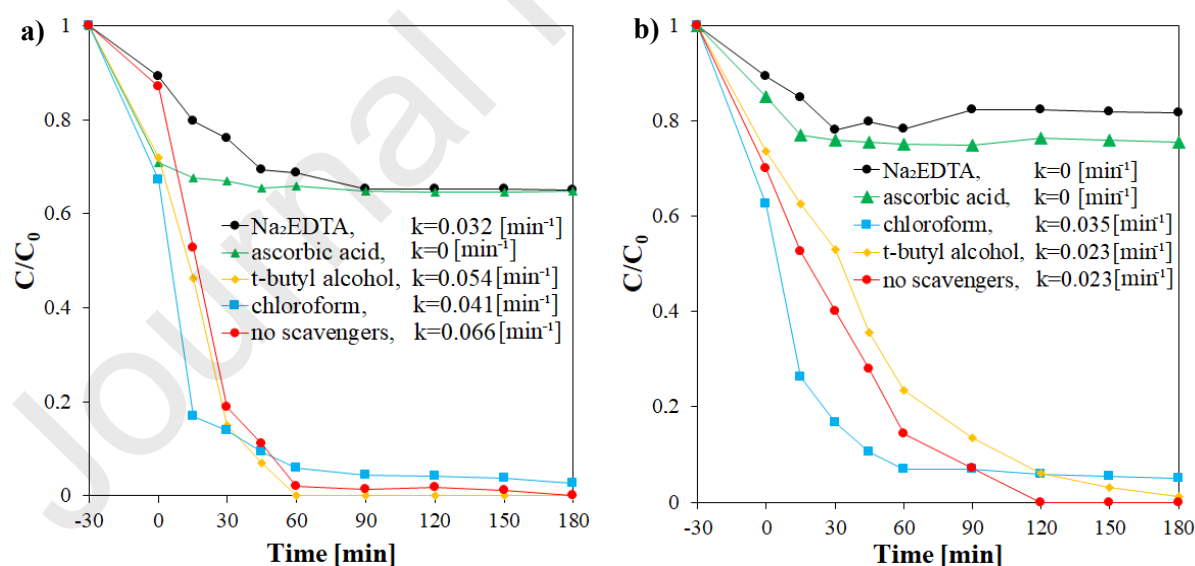

Figure 9. Degradation of IMA with and without scavengers under a) sunlight and b) visible light in the presence of BiOCl1.3Br0.7

Para-benzoquinone and ascorbic acid were used as a scavengers to study the role of $^{\bullet}O_2^{-}$ in the removal of 5-FU and IMA, respectively [43]. Considerable inhibition of both cytostatic drugs was observed in presence of these scavengers in simulated solar and visible light irradiation. The fact confirmed that $^{\bullet}O_2^{-}$ is one of the main oxidants in photodegradation of drugs under BiOCl1.3Br0.7. However, the role of $^{\bullet}O_2^{-}$ radicals in the decomposition process was to more extent in case of IMA than 5-FU. Previous reports on cytostatic drugs removal in the presence of $BiOCl_{0.5}Br_{0.5}$ solid solution under UV-vis light showed that 5-FU was mainly oxidized by h^{+} while IMA by $^{\bullet}O_2^{-}$ entities [23]. $^{\bullet}O_2^{-}$ radicals generated by the illumination of BiOCl was identified as the main species responsible for decomposition of pharmaceuticals such as carbamazepine and ciprofloxacin when exposed to simulated sunlight [43, 44].

In order to determine the involvement of electrons and secondary $^{\bullet}OH$ radicals in decomposition of 5-FU and IMA, chloroform and *tert*-butyl alcohol as scavengers were used, respectively [43,44]. The effect of addition of chloroform and *tert*-butyl alcohol on the 5-FU degradation rate under both types of light irradiation was minor but observable. The results confirmed that $^{\bullet}OH$ radicals were absent in the system under solar light, but it could slightly participate in 5-FU degradation under visible light. The e^{-} had a some role in the 5-FU degradation especially under visible light. The degradation rate of IMA in the presence of *tert*-butyl alcohol was unchanged, while the addition of chloroform accelerated the process. On the second hand, the addition of the Na_2EDTA holes scavenger [23, 43] dramatically reduced the degradation rate of both studied anticancer drugs proving that h^{+} mediated oxidation process was the predominant pathway leading to degradation of 5-FU and IMA under solar and visible light. The results were consistent with literature reports suggesting that the BiOX photocatalyst generated h^{+} and $\bullet O_2^{-}$ and that these species were important in the photocatalytic removal of pharmaceuticals. [23, 43, 44]. These findings explained the elevation of IMA degradation in presence of chloroform by the improve separation of photogenerated charge pairs e^{-}/h^{+} onto photocatalyst surface.

Summarizing, in the presence of BiOCl1.3Br0.7 IMA was removed faster from the single drug solution than 5-FU In the decomposition processes of both drugs the same species were participated. The key pathway of IMA degradation proceeded through h^{+} and $^{\bullet}O_2^{-}$ attack reaction, while in the 5-FU degradation the key role played h^{+} and following in less extend $^{\bullet}O_2$. The e^{-} and secondary $^{\bullet}OH$ radicals could also participated in 5-FU decomposition especially under visible light.

3.3.5. The effect of foreign species in decomposition of 5-FU

3.3.5.1. Photocatalytic removal of 5-FU with and without of IMA as foreign species

The effect of foreign organic matter in decomposition of 5-FU in the 5-FU/IMA mixture was investigated for BiOCl1.3Br0.7 photocatalyst and compared with results for a single solution of 5-FU and IMA drugs.
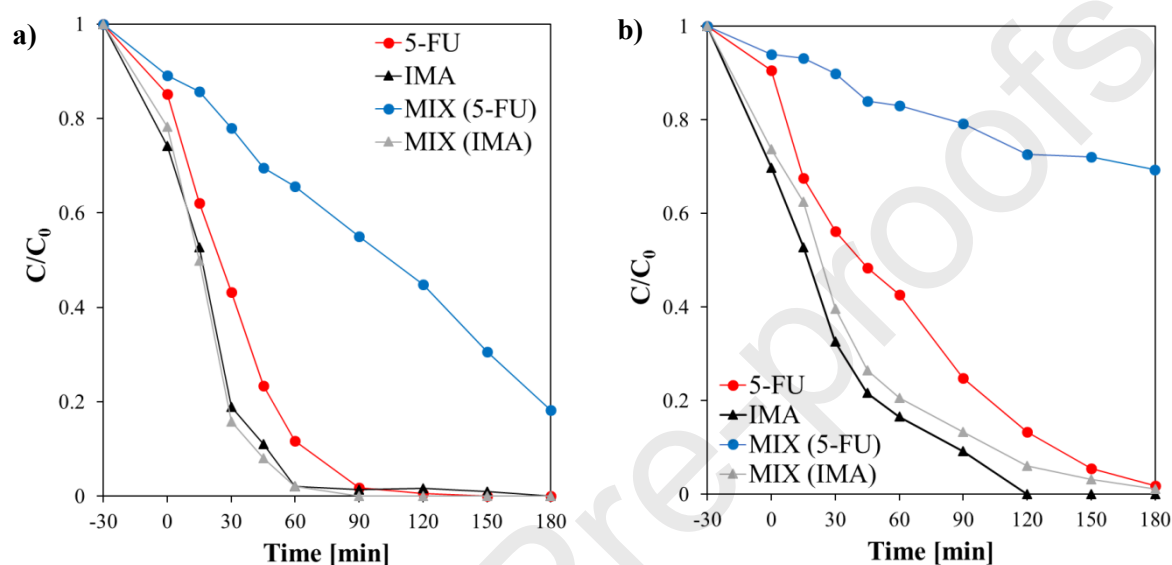

Figure 10. Photocatalytic simulltaneus degradation of 5-FU and IMA under a) solarlight and visible light irradiation.

As shown in Figure 10a, the addition of 15 mg L^{-1} IMA to solution of 15 mg L^{-1} 5-FU led to a five times slower degradation rate of 5-FU (decrease from k_{app}= 0.050 min^{-1} to k_{app}=0.008 min^{-1}) (Figure 11b), while the IMA removal rate in the presence of 5-FU was only slightly changed (from k_{app}=0.066 min^{-1} to 0.061 min^{-1}).

After 60 minutes of solar light irradiation, the removal of IMA was almost complete in both the 5-FU/IMA mixture and individual treatment. After 90 min of 5-FU photodegradation the efficiency was 100% in the single drug solution, while this value dropped down to 45% in the drugs mixture.

In visible light the trend in IMA and 5-FU treatment was similar as in simulated solar light irradiation. The removal of IMA was complete in 120 min in both the single drug solution and in the mixture. The efficiency of 5-FU removal dropped from 100%, when treated individually to 31% in mixture of 5-FU/IMA. The value of 5-FU degradation rate (k_{app}=0.002 min^{-1}) was

ten times slower in mixture than the value of k_{app} obtained, when the drug was decomposed in its singly solution (k_{app} = 0.020 min^{-1}). The value of k_{app} for IMA was 0.023 min^{-1} for both the single drug solutions and for the mixture degradation.

The total concentration of organic compounds in mixture was 30 mgL^{-1}, while the concentration in single drug solution was 15 mgL^{-1}. The increase of organic matter content in the mixture slowed down the rate of drugs degradation. However the inhibition extent for drugs was different due to their various chemical structure.

The results suggested that 5-FU and IMA competed for the photogenerated h^{+} and $^{\bullet}O_2^{-}$ species. IMA as a higher molecule size compound with three aromatic rings was mainly target of these species. Therefore, in the presence of IMA the available amount of active entities participating in 5-FU degradation decreased, and the degradation rate slowed down.

The effectiveness of TOC removal in both single drug solutions and in the mixture was very low (Figure 11a).
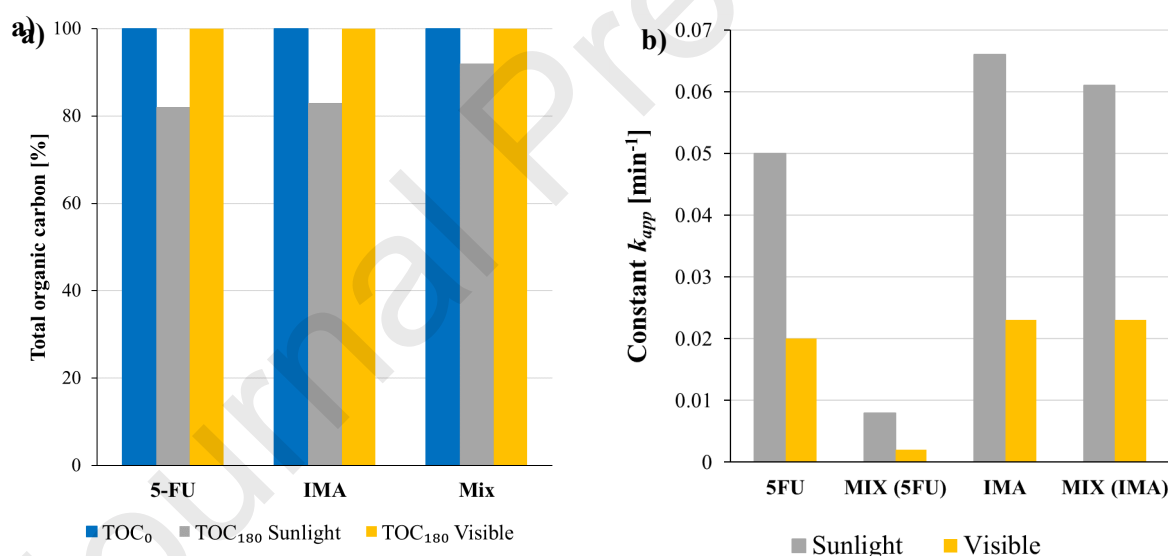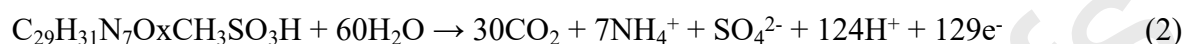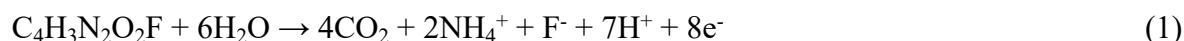

Figure 11 a) Total organic carbon (TOC) removal and b) rate constant k_{app} of cytostatic drugs decomposition after 180 min. of BiOCl1.3Br0.7 illumination in single drug solution (5-FU, IMA) and in their mixture MIX(5-FU), MIX(IMA).

Under simulated solar light TOC removal in 5-FU and IMA solution reached 17 and 18%, respectively. As expected in the 5-FU/IMA mixture, the TOC removal efficiency was even lower (8%). TN removal either in the single drug solutions as well as in the mixture of drugs

was not noticed. Visible light did not lead to the mineralization of individual drugs and their mixture, therefore the TOC and TN values did not change after photocatalysis. The nitrogen atoms built-in organic matter were to low extent released into the solution in the form of ammonium ions.

Mineralization process of 5-FU and IMA can be presented by the following reactions:

$$C_4H_3N_2O_2F + 6H_2O \rightarrow 4CO_2 + 2NH_4^+ + F^- + 7H^+ + 8e^- \tag{1}$$

$$C_{29}H_{31}N_7OxCH_3SO_3H + 60H_2O \rightarrow 30CO_2 + 7NH_4^+ + SO_4^{2-} + 124H^+ + 129e^- \tag{2}$$

According to reactions (1) and (2), mineralization of 15 mg of IMA theoretically required transfer of 3,6 times more electrons to the acceptor (h^+) than 15 mg L^{-1} of 5-FU. However, in our experimental conditions, the efficiency of 5-FU mineralization was as low as IMA. This suggested that intermediates photogenerated during 5-FU decomposition were much less sensitive in photocatalytic oxidation than the intermediates of the IMA degradation. Based on the pH decrease from 6.3 to 5.3 after 180 min of 5-FU photocatalysis, it can be concluded that carboxylic acids appeared as by-products.

3.3.6 Influence of inorganic ions naturally exist in waterbodies on the 5-FU and IMA decomposition

The inorganic ions naturally existing in the waterbodies may affect the kinetics of pollutants degradation during photocatalysis [45, 46]. The influence of the anions including Cl^-, SO_4^{2-}, HCO_3^-, and NO_3^- in concentration of 3mM on the 5-FU photocatalytic degradation under simulated solar and visible light irradiation was shown in Figure 12.
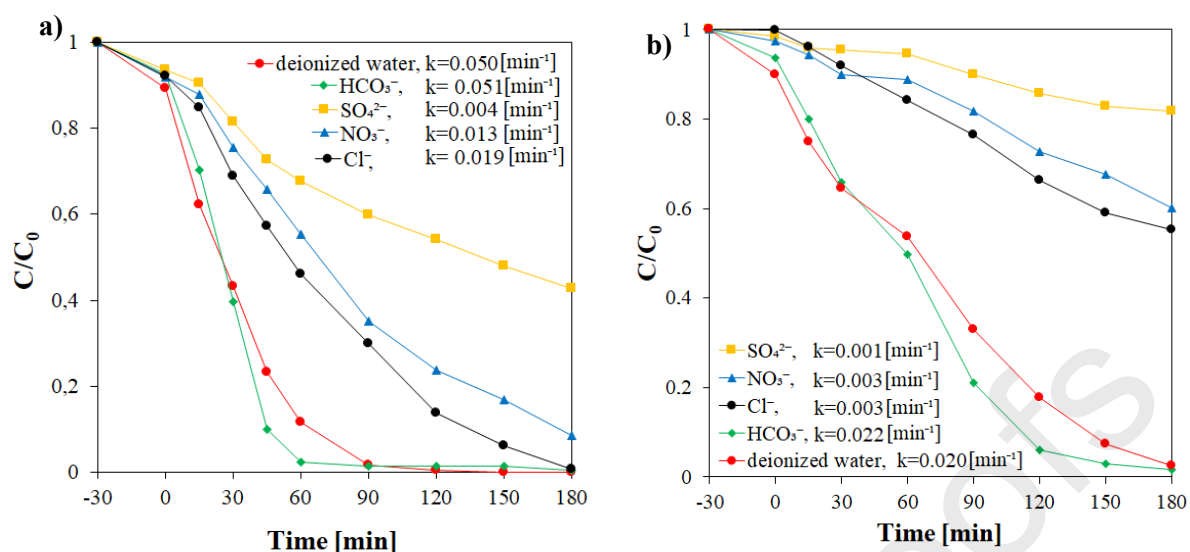
Figure 12. Degradation of 5-fluorouracil ions enriched water under a) artificial solar and b) visible light.

The concentration of ions was higher than that in municipal wastewater [22], therefore, if the ion had any negative effect on photocatalysis this could be observed.

In the dark phase the all examined anions had an insignificant effect on the efficiency of 5-FU removal in the single drug solution, while in the light phase the values of k_{app} of 5-FU oxidation decreased in following order $k_{app}(HCO_3^-) > k_{app}(\text{without ions}) > k_{app}(Cl^-) > k_{app}(NO_3^-) \geq k_{app}(SO_4^{2-})$. The trend in inhibition of 5-FU degradation by anions was similar regardless of the type of light, but the suppression was higher in visible light.

The negative impact of Cl^-, NO_3^- and SO_4^{2-} anions may be caused by their adsorption at the photocatalyst surface, due to the presence of Bi-OH_2^+ at pH 6.3 (experimental conditions), blocking free active centers capable to organic matter oxidation. For SO_4^{2-} ions BiOCl1.3Br0.7 photocatalyst had stronger adsorption and reduced the reaction sits due to the double charge and larger molecular size than other applied anions. The other possible mechanism of inhibition of 5-FU oxidation could be the quenching of h^+ by SO_4^{2-} and Cl^- according to reaction (3), and the increase in the production of the more selective (e.g. $SO_4^{2-\bullet}$, $Cl^\bullet$) and weaker oxidants by depressing the amount of powerful oxidants (h^+)

$$\text{Anion}^{n-} + h^+ \rightarrow \text{Anion}^{(n-1)-\bullet} \qquad (3)$$
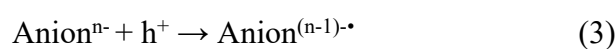
The higher inhibition extent in presence of SO_4^{2-} than Cl^- suggested that $^\bullet SO_4^{2-}$ radicals generation was doubtful [47]. The adsorption of SO_4^{2-} and Cl^- on the photocatalyst surface was probably the main process that led to inhibition of drug removal.

The less NO_3^- ions effect was found, whereas HCO_3^- ions accelerated the degradation of 5-FU. This fact confirmed our assumption that adsorption played the main role in inhibiting 5-FU degradation. NO_3^- and HCO_3^- ions were rather weak h^+ scavengers, but they could cause some kind of shielding effect for irradiations. Two phenomena for shielding effect were possible: the adsorption of anions could block the number of active sites responsible for cytostatic drug oxidation, and NO_3^- and HCO_3^- could act strongly as an UV absorber. In the second case the secondary $^{\cdot}OH$ radicals could be produced. These entities are known as very effective oxidants of 5-FU in bulk solution, and can mitigate the effects of inhibition of 5-FU oxidation [40]. In our case, however, NO_3^- ions inhibited 5-FU degradation more significantly than Cl^-, therefore $^{\cdot}OH$ radicals formation was doubtful. Whereas, HCO_3^- ions enhanced the photocatalytic degradation of 5-FU. The results of the terephthalic acid (TA) experiment showed that •OH radicals were not formed in the presence of these ions in our conditions. This indicated that the long-lived bicarbonate radicals could participate in 5-FU decomposition, but the further study to explain this phenomenon is needed.

In the next step the experiment for the mixture of 5-FU/IMA was performed. The inorganic anions were added in the same amount as before. The influence of them on 5-FU adsorption was low, but the effect on removal of IMA was extremely significant as shown in Figure 13.
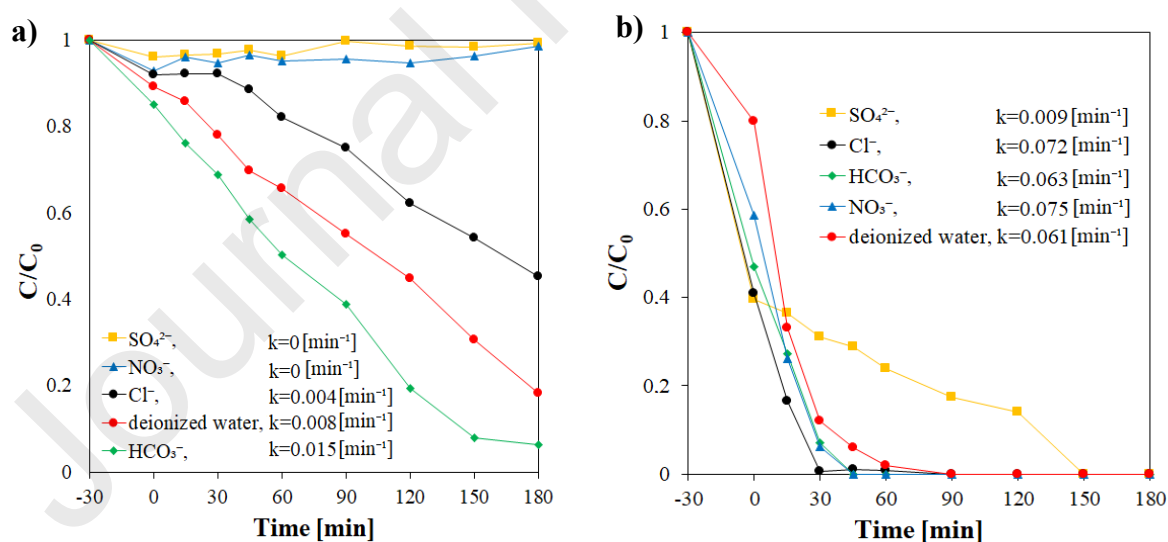

Figure 13. Influence of inorganic ions on a) 5-fluorouracil and b) imatinib when drugs were as a mixture.

In the presence of anions the adsorption of IMA at photocatalyst surface was strongly elevated up to 42-72%. Due to the applied pH 6.4, IMA exist as a cation $IMAH^+$, while the photocatalyst

surface received negative character by anions adsorption. The electrostatic attraction between the negatively charged surface and the positively charged drug molecule resulted in an increased in the dark phase adsorption. Moreover, the attractive effects between the photocatalyst surface and the IMAH$^+$, proved that anions were located on the photocatalyst surface.

In the light phase, SO_4^{2-} and NO_3^- ions totally inhibited 5-FU degradation in 5-FU/IMA mixture. The higher inhibition of 5-FU degradation in the mixture than in single drug solution could be induced by the additive effect of IMA and inorganic anions. The results confirmed that photoadsorption of IMA on BiOCl1.3Br0.7 was related with an electrostatic (IMAH$^+$ and negatively charged photocatalyst surface) controlling factor, while 5-FU with the pyrimidine ring could prefer hydrophobic interaction. Therefore, IMA occupied the active sites on the photocatalyst surface, while 5-FU had limited access to them.

Under light irradiation the anions applied, except SO_4^{2-} insignificantly affected IMA removal. Moreover, the kinetics of IMA decomposition in the presence of SO_4^{2-} ions changed from pseudo-first order reaction to zero order reaction, which rate likely only depended on the intensity of the incident radiation. In the presence of inorganic ions, the mineralization of drugs in the single drug solution and in their mixture was not found.

As shown in Fig. 14 the influence of the Ca^{2+}, Fe^{3+} and Ag^+ cations on degradation of 5-FU in single drug solution under simulated sunlight irradiation was also investigated.
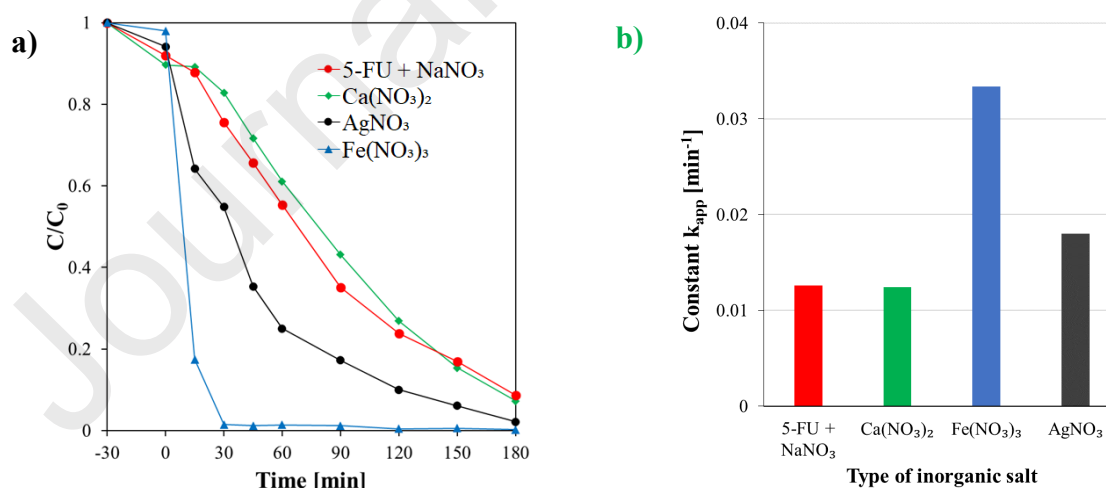

Figure 14. a) Influence of inorganic cations on degradation of 5-FU b) and the rate constant k_{app} of 5-FU degradation under artificial solar light.

The investigations of anions effect on the degradation rate of drug, have shown that they slowed down the rate of drug degradation. To observe only the cation effect, all studied cations were used as nitrates and the results were compared with the drug degradation rate in the presence of $NaNO_3$.

Fe^{3+} and Ca^{2+} are the cations naturally exist in the waterbodies, where they are responsible for the water hardness. Ca^{2+} ions exhibited no effect on the 5-FU degradation. The positively charged Ca^{2+} in the 5-FU solution were repulsed with the positive charged BiOCl1.3Br0.7 surface and the h^+ in active centers were fully available for drug. Fe^{3+} ions improved photocatalytic activity of studied photocatalyst. It can be explained by two phenomena. Firstly, Fe^{3+} could act as an electron scavenger, resulting in higher separation of photogenerated charge pairs h^+/e^- and higher availability of holes in the 5-FU decomposition process. Secondly, Fe^{3+} could participate in Fenton-like reaction (Equation 4,5) producing additional strong oxidants - hydroxyl radicals, which were effective in organic matter decomposition in solution.

$$O_2 + e^- \rightarrow {}^{\bullet}O_2^- + H^+ \rightarrow HO_2^{\bullet} \rightarrow \rightarrow H_2O_2 \qquad (4)$$

$$Fe^{3+} + H_2O_2 \rightarrow Fe^{2+} + HO_2^{\bullet} + H^+ \qquad (5)$$

The Ag^+ ions just like Fe^{3+} accelerated the 5-FU degradation rate but in a less extent. Ag^+ ions are pollutants, which scavenging of ${}^{\bullet}O_2^-$ radicals, and can permanently modify photocatalyst surface [48]. Due to the BiOCl1.3Br0.7 sample was able to produce of superoxide, Ag^+ ions could be reduced by these entities to Ag-metal nanoparticles and immobilized on the photocatalyst surface. This resulted in a better separation of photogenerated charges pairs e^-/h^+, and hence an increase in photocatalytic activity. The concentration of Fe^{3+} and Ag^+ cations in the waterbodies and wastewater is much lower than the 3 mM used in the study. However, if the photocatalyst was used in flow system their impact on the organic matter removal rate could be observed.

Research of photocatalyst stability was an important aspect of developing of a material. Thus, the efficiency of BiO1.3Br0.7 sample in four consecutive photocatalytic cycles was investigated. (Figure 15).
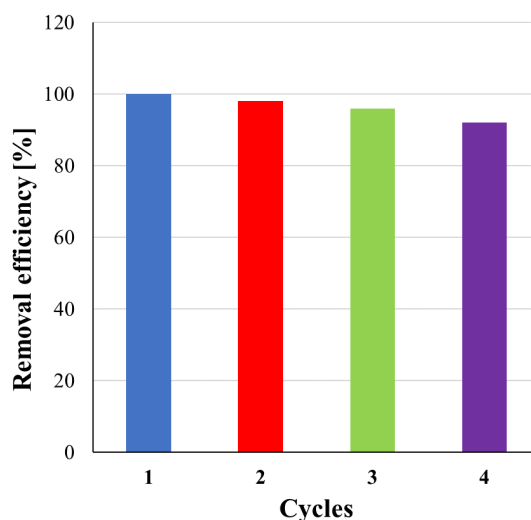
Figure 15. The photocatalytic stability of BiO1.3Br0.7 during 5-FU removal in single drug solution under solar light irradiation.

5-FU degradation efficiency in fourth cycle in the presence of BiO1.3Br0.7 irradiated by solar light was reduced to 92% of first cycle efficiency. These results clearly showed good stability of prepared material over four consecutive cycles.

3.3.7. The pathway degradation of 5-FU and IMA under artificial solar and visible light

In order to identify the 5-FU and IMA intermediates photogenerated over BiOCl1.3Br0.7 in the studied system, the solution samples collected with progress of photocatalysis, were analyzed by LC-MS in both the positive and negative ionization mode. Based on the accurate mass measurements as well as on characteristic mass fragments, the possible intermediates structures were proposed.

The degradation of 5-FU by photocatalysis led to the formation of five and seven intermediates (FUs) for simulated solar and visible light irradiation, respectively. Positive and negative ionization was used, but the only negative ionization get the main [M - H]⁻ FUs. Total ion current (TIC) chromatograms of drug degradation under solar light at different times in negative mode and selected intermediates MS2 spectrograms were presented in Fig S.1 and Table S1 (Supplementary material).

Some of FUs were identified for the first time for the 5-FU decomposition in heterogeneous photocatalysis. The probably pathway of 5-FU decomposition in the presence of BiOCl1.3Br0.7 was presented in Fig. 16.
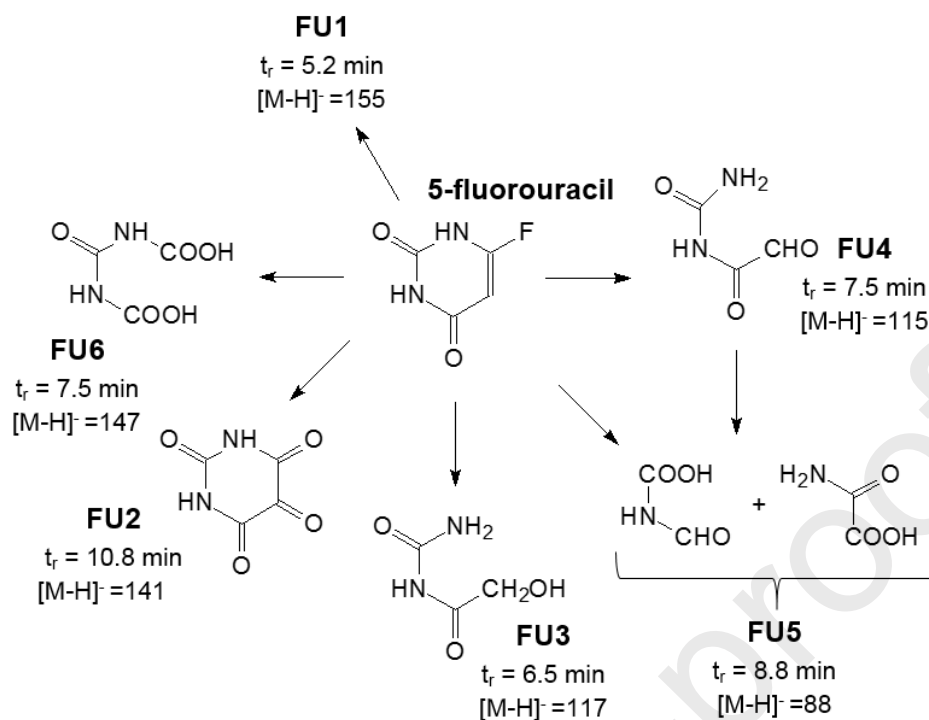
Figure 16. Possible photocatalytic degradation pathway of 5-fluorouracil.

According to the kinetic profiles under solar light irradiation depicted in Figure 17 the increase of FU1-FU4 intermediates formation was observed, attaining a maximum area at 45 min.
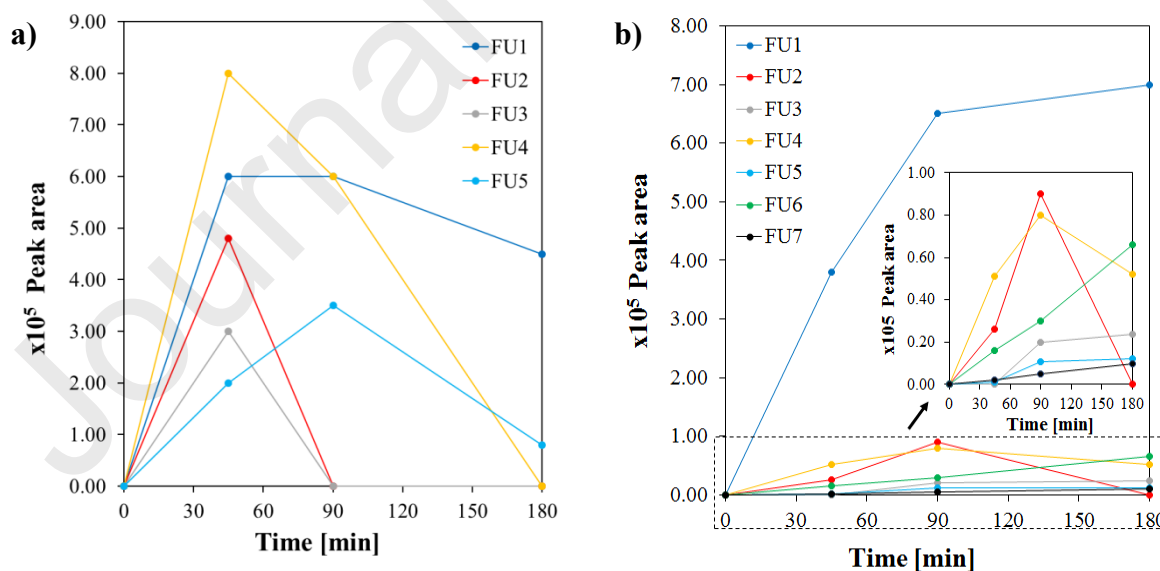

Figure 17. Kinetic profiles of 5-FU intermediates formation under a) solar and b) visible light

Then their area were decreasing, suggested that intermediates formed in the first stage were further decomposed. In contrast, under visible light irradiations, a slower production of FU2-

FU7 was found and, the peaks area of the intermediates was much smaller. Moreover, with the progress of photodegradation the area of peaks gradually increased, which suggested that the progress of photocatalytic degradation of 5-FU was less advanced under visible light.

The results obtained in the scavenger experiments indicated direct oxidation by h^+ of 5-FU over BiOCl1.3Br0.7 under simulated solar light irradiation as the major pathway of drug degradation. Dhananjeyan [49] reported that the oxidation of 5-FU by h^+ is followed by a loss of an electron from the C5-C6 double bond of pyrimidine ring leading to radical cation intermediates. These intermediates react with H_2O leading to hydroxyl-derivatives, similar as those formed by the $^\bullet OH$ radicals attack. It is the reason that the intermadiates found were similar to those found in other advanced oxidation processes.

Defluorination of 5-FU in the presence of BiOCl1.3Br0.7 could occur as a consequence of reaction with photogenerated e^- (reaction 6 and 7).

$$BiOCl_nBr_m/Bi_4O_5Br_2 + h\gamma \rightarrow (VB)h^+ + (CB)e^- \qquad \text{photocatalyst activation (6)}$$

$$5\text{-}FU + (CB)e^- \rightarrow 5\text{-}FU^{+\bullet} + F^- \qquad \text{defluorination (7)}$$

The 5-FU could be oxidized by the valence band holes (h^+) or reduced by conducting band e^- that subsequently lead to the defluorination, hydroxylation (FU2, $[M-H]^- = 141$) and further to breakup of previous intermediate structure into various fragments (FU3-FU7, $[M-H]^- = 117$, 115, 88, 147, 104). If reductive defluorination of 5-FU has occurred in the presence of BiOCl1.3Br0.7, O_2 which reacts with $(CB)e^-$ yielded $^\bullet O_2^-$, could inhibit drug decomposition by competition. The results of experiments carried out under air-equilibrium conditions and with introduction of oxygen into the system showed that 5-FU decomposition was impeded in the presence of oxygen access (data not shown). This fact proved that partially degradation through defluorination of 5-FU occurring by direct reaction with $(CB)e^-$ and that $^\bullet O_2^-$ radicals are less important than h^+ in the drug degradation.

Summarizing hydroxylated derivatives FU2 of defluorinated 5-FU were formed by direct oxidation and hydrolysis, while their fragmentation led to the occurrence of FU3 – FU7 (Fig. 17).

The applied processes to IMA degradation in solar and visible light irradiation proceeded through seven main intermediates (IMs). Positive and negative ionization was used, but the only positive ionization get the main $[M + H]^+$ IMs. Total ion current (TIC) chromatograms of drug degradation under solar light at different times in positive mode for IMA and selected intermediates MS2 spectrograms were presented in Fig S2 and Table S2 (Supplementary material).

There were found three IMs with $[M+H]^+=510$ at the different retention time (tR) (IM1(510); IM2(510); IM3(510)) and $[M + H]^+ = 340$ (IM6); 277 (IM7); 234.5 (IM5); 235.5 (IM4). IM1, IM2 and IM3 (510) corresponded to mono-oxidation products of IMA, produced by hydroxylation pathway. According to the fragmentation pattern, the hydroxylation was proposed on one of the N atoms of N-methyl-piperazin in the IMA molecule forming the IM2 and IM3, while IM1 could be obtained by hydroxylation of the -CH$_3$ group in 4-methylpiridine in IMA structure. $[M + H]^+ = 340$; 277; 234.5 and 235.5 were formed by the cleavage of the N-C bonds in the IMA molecule (Fig. 18). The main intermediates were illustrated in Figure 18.
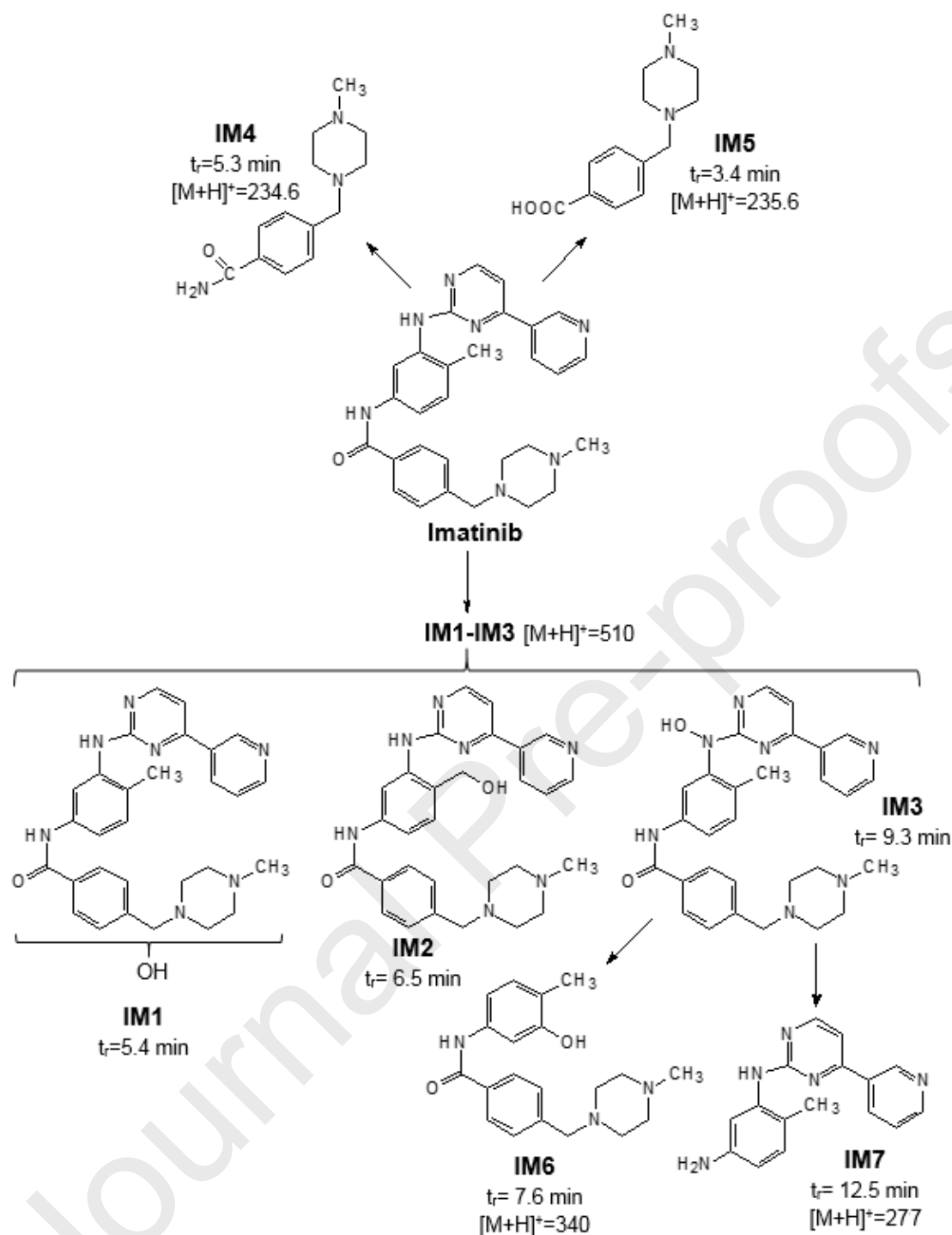
Figure 18. Photocatalytic degradation pathway of IMA.

According to the kinetic profiles under simulated solar light, the degradation of by-products simultaneously with IMA elimination could be observed (Fig. 19). Under visible light irradiation the IMA degradation led to more amount of intermediates. Moreover, with progress of photocatalysis an increase of the areas of IMs peaks were observed (exception IM7), which

confirmed that the IMA decomposition occurred to a lesser extent under visible light than simulated solar light.
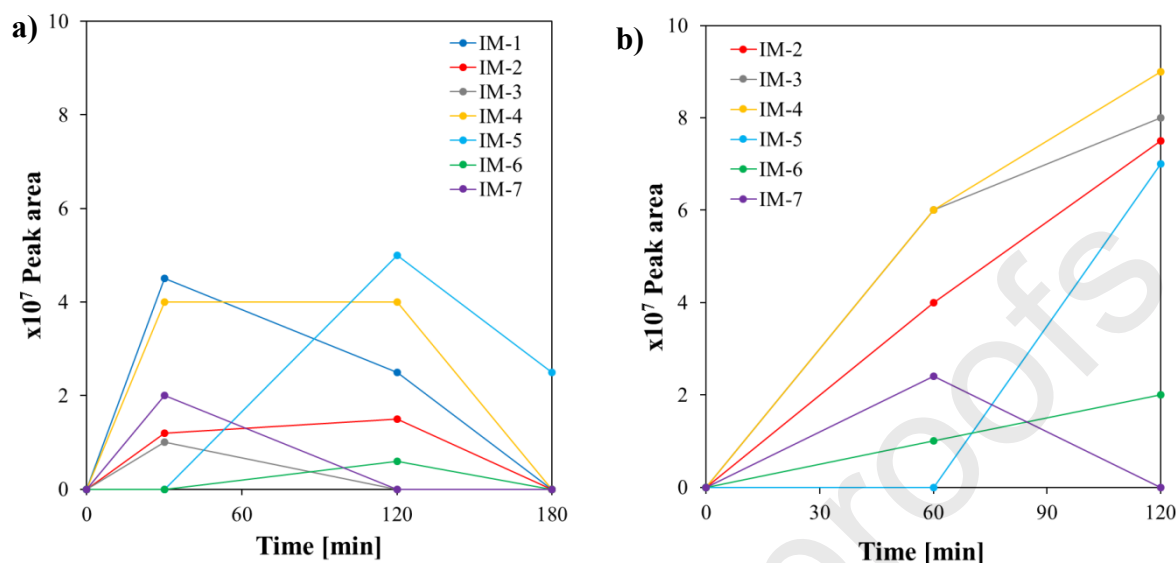
Figure 19. Kinetic profiles of IMA intermediates formation under a) solar and b) visible light.

It was reported that the main degradation products under photolytic conditions were 4-methyl-N3-(4-pyridin-3-yl-pyrimidyn-2-yl)-benzene-1,3-diamine (IM7, [M+H]+=277) and 4-(4-methyl-piperazin-1-ylmethyl)-benzoic acid (IM4, [M+H]+=235.5), while the main degradation products under oxidation conditions, were 4-[(4-methyl-4-oxido-piperazin-1-yl)-methyl]-N-[4-methyl-3-(4-pyridin-3-yl-pyrimidin-2-ylamino)-phenyl]-benzamide ([M+H]+=510), 4-[(4-methyl-1-oxido-piperazin-1-yl)-methyl]-N-[4-methyl-3-(4-pyridin-3-yl-pyrimidin-2-ylamino)-phenyl]-benzamide (MI1) and 4-[(4-methyl-1,4-dioxido-piperazin-1-yl)-methyl]-N-[4-methyl-3-(4-pyridin-3-yl-pyrimidin-2-ylamino)-phenyl]-benzamide. IM1-IM3 (([M+H]+=510), IM4 and IM7 were also found in our study, but the localization of -OH functionalities in IM1-IM3 seems to be different than in other investigations [50].

3.4 Toxicity

All studied drugs in single drug solutions and in mixture of 5-FU/IMA had toxic effect on the test organism limiting its growth (Figure 20a). The EC_{50} values showed that the highest toxicity was observed for the mixture of both drugs, i.e. 3.5 ± 0.2 mg L^{-1}, whereas for the drugs individually EC_{50} was significantly lower (ANOVA, $p<0.05$; Tukey HSD test, $p<0.05$) and it was $20.6+1.4$ mg L^{-1} for 5-FU and $6.2+0.4$ mg L^{-1} for IMA). At the highest concentration of 5-FU and IMA (50 mg L^{-1}) the growth rate of *C. vulgaris* was reduced by 71% and 90%, respectively. The growth inhibition of the green alga at the drug concentration of 15 and 30 mg

L^{-1} was higher for imatinib (85%) compared to 5-FU (40 and 66% respectively) (ANOVA, p<0.05; Tukey HSD test, p<0.05). The mixture of IMA/5-FU at the concentration of 30 mg mL^{-1} (15+15 mg L^{-1}) further significantly increased the toxicity of the solution almost completely inhibiting the growth of the test organism (94%), indicating the existence of synergistic effect of some sort.

The photooxidation process under simulated solar irradiation and in the presence of BiOCl1.3Br0.7 sample significantly reduced the toxic effect of both drugs and their mixture (ANOVA, p<0.05; Tukey HSD test, p<0.05). Obtained data did not allow calculating EC$_{50}$ values. For the most of the applied concentrations of oxidation mixtures their inhibitory effect reached up to 20% (data not shown). Higher growth reduction was only observed when the growth of *C. vulgaris* was tested directly in undiluted oxidation mixtures (Fig. 20b). The mixture of intermediates obtained from the oxidation of 5-FU (15 mg L^{-1}) limited the growth of the alga by 39%. For the mixture of intermediates produced by IMA alone (15 mg L^{-1}) and 5-FU/IMA mixture (15+15 mg L^{-1}) degradation the growth inhibition was ca. 3.3 times lower compared to IMA and 5-FU/IMA before photooxidation.
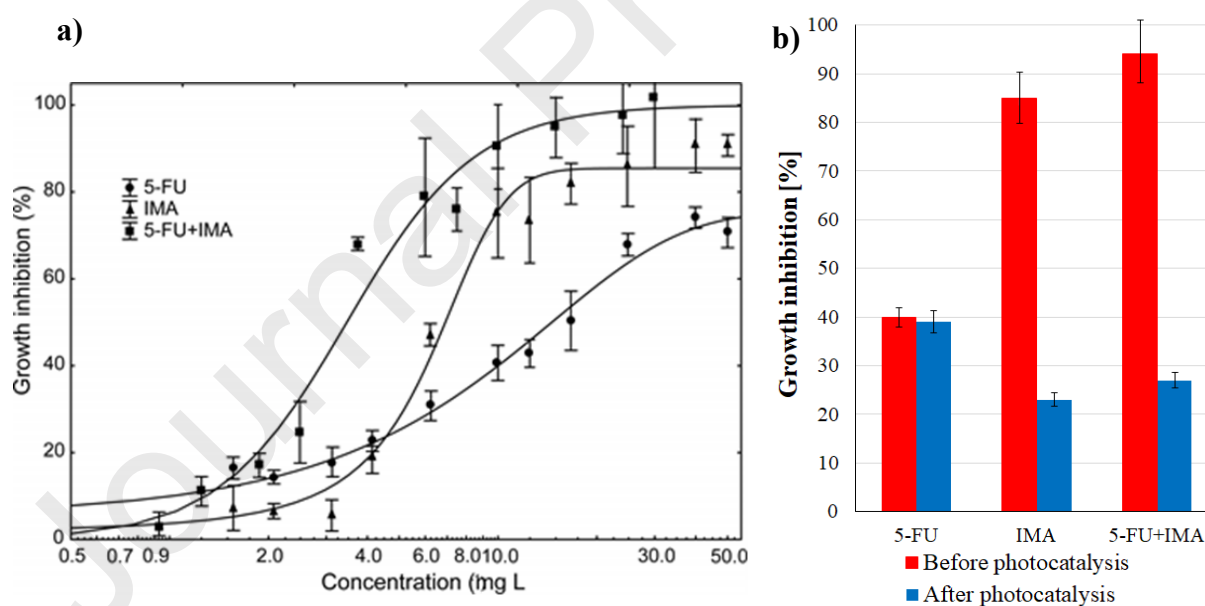
Figure 20 a) Toxicity tests on Chlorella vulgaris exposed to 5-fluorouracyl (5-FU; 50 mg L-1), imatinib (IMA; 50 mg L-1), their combination (5-FU/IMA; 15+15 mg L-1). Data are means±SD presented as dose-response curves of growth inhibition after 96-h exposure. b) Effect of photocatalysis on growth inhibition of *Chlorella vulgaris* after 96-h exposure to 5-fluorouracyl (5-FU; 15 mg L^{-1}), imatinib (IMA; 15 mg L^{-1}), their combination (5-FU/IMA; 15+15 mg L^{-1}) oxidation mixtures.

4.   Conclusions

The present work investigated the synthesis of series of $BiOCl_nBr_m$ where the molar Cl/Br ratio was 2/0, 1.9/0.1; 1.5/0.5; 1.3/0.7; 0.7/1.3; 0.5/1.5; 0/2, and its characterization including photocatalytic activity for the removal of cytostatic drug 5-FU under UV-Vis light irradiation. The activity of $BiOCl_nBr_m$ did not correlate with the BET specific surface area, decreasing when *m* dropping from 2 to 0. The best activity in 5-FU removal characterized BiOCl1.3Br0.7. The dose of 200 mg L^{-1} of photocatalyst was enough to completely removal of the studied drug. The influence of pH was insignificant under acidic conditions, while the degradation effect of 5-FU significantly decreased at alkaline pH.

Further, BiOCl1.3Br0.7 sample was applied to 5-FU treatment in presence of other cytostatic drug IMA, the inorganic anions and cations naturally existed in waterbodies and wastewater under simulated solar and visible light irradiation. Both cytostatic drugs singly and in their mixture were insignificantly removed by direct solar and visible photolysis, and their adsorption in dark phase on the photocatalyst surface was also marginal. The fact revealed that the photodegradation of cytostatic drugs was mainly occurred by photooxidation.

The background entities existed in natural water such as Cl^-, SO_4^{2-}, HCO_3^-, and NO_3^- influenced on the degradation effect of studied drugs process. The anions inhibited 5-FU degradation mainly by occupying of active centers, except bicarbonate ions, which activated by light could react with 5-FU accelerating its decomposition. The Fe^{3+} and Ag^+ cations elevated the degradation rate of 5-FU.

The mechanism of photocatalytic degradation of 5-FU and IMA was investigated by scavenging experiments and identification of by-products under simulated solar and visible light. Scavenging studies proved that h^+ and $^•O_2^-$ are responsible for the major degradation of 5-FU and IMA. However h^+ played the most significant role in 5-FU removal, while $^•O_2^-$ in IMA treatment. The photogenerated e^- can also participate in defluorination of 5-FU.

The transformation of 5-FU and IMA proceeded through the formation from seven to five intermediates involving hydroxylation, oxidative cleavage, hydrolysis pathways and reductive defluorination of 5-FU.

The toxicity towards *Chlorella vulgaris* for the parent 5-FU, IMA, when they were individually and in their mixture was observed. After 3 h of photocatalytic degradation under simulated solar light irradiation toxicity decreased 2.0, 3.3 and 3.3 times for 5-FU, IMA and 5-FU/IMA, respectively. The decrease of toxicity was the highest in the mixture of drugs.

The results suggested that the photocatalytic treatment over $BiOCl_nBr_m$ is a promising method for cytostatic drugs removal from water.

Acknowledgment

References

[1] R. Hirsch, T. Ternes, K. Haberer, K.L. Kratz, Occurrence of antibiotics in the aquatic environment, Sci. Total Environ. 225 (1999) 109-118. https://doi.org/10.1016/S0048-9697(98)00337-4.

[2] M.D. Hernando, M. Mezcua, A.R. Fernandez-Alba, D. Barcelo, Environmental Risk Assessment of Pharmaceutical Residues in Wastewater Effluents, Surface Waters and Sediments, Talanta, 69 (2006) 334-342. https://doi.org/10.1016/j.talanta.2005.09.037.

[3] T.A Ternes, Occurrence of drugs in German sewage treatment plants and rivers, Water Res. 2 (1998) 3245-3260. https://doi.org/10.1016/S0043-1354(98)00099-2.

[4] S. Santana-Viera, P. Hernandez-Arencibia, Z. Sosa-Ferrera, J.J Santana-Rodriguez, Simultaneous and systematic analysis of cytostatic drugs in wastewater samples by ultra-high performance liquid chromatography tandem mass spectrometry, J. Chromatogr. B, 1110-1111 (2019) 124-132. https://doi.org/10.1016/j.jchromb.2019.02.018.

[5] J.O. Straub, Combined Environmental Risk Assessment for 5-Fluorouracil and Capecitabine in Europe, Integr. Environ. Assess. 6 (2009) 540-566. https://doi.org/10.1897/IEAM_2009-073.1.

[6] J.P Besse, J.F Latour, J. Garric, Anticancer drugs in surface waters: What can we say about the occurrence and environmental significance of cytotoxic, cytostatic and endocrine therapy drugs?, Environ. Int. 39 (2012) 73-86. https://doi.org/10.1016/j.envint.2011.10.002.

[7] V. Booker, C. Halsall, N. Llewellyn, A. Johnson, R. Williams, Prioritising anticancer drugs for environmental monitoring and risk assessment purposes, Sci. Total Environ. 473-474 (2014) 159-170. https://doi.org/10.1016/j.scitotenv.2013.11.145.

[8] M.S.F. Santos, H. Franquet-Griell, S. Lacorte, L.M Madeira, A. Alves, Anticancer drugs in Portuguese surface waters-Estimation of concentrations and identification of potentially

priority drugs, Chemosphere 184 (2017) 1250-1260. https://doi.org/10.1016/j.chemosphere.2017.06.102.

[9] P.H. Secretan, M. Karoui, H. Sadou-Yaye, Y. Levi, L. Tortolano, A. Solgadi, N. Yagoubi, B. Do, Imatinib: Major photocatalytic degradation pathways in aqueous media and the relative toxicity of its transformation products, Sci. Total Environ. 655 (2019) 547-556. https://doi.org/10.1016/j.scitotenv.2018.11.270.

[10] M. Akkari, P. Aranda, C. Belver, J. Bedia, A.B.H Amara, E. Ruiz-Hitzky, Reprint of ZnO/sepiolite heterostructured materials for solar phocotacalytic degradation of pharmaceuticals in wastewater, App. Clay Sci. 160 (2018) 3-8. https://doi.org/10.1016/j.clay.2018.02.027.

[11] S. Teixeira, R. Gurke, H. Eckert, K. Kuhn, J. Fauler, G. Cuniberti, Photocatalytic degradation of pharmaceuticals present in conventional treated wastewater by nanoparticle suspensions, J. Environ. Chem. Eng. 4 (2016) 287-292. https://doi.org/10.1016/j.jece.2015.10.045.

[12] I. Oller, S. Malato, J.A Sánchez-Pérez, Combination of Advanced Oxidation Processes and biological treatments for wastewater decontamination - A review, Sci. Total Environ. 409 (2011) 4141–4166. https://doi.org/10.1016/j.scitotenv.2010.08.061.

[13] S. Carbonaro, M.N Sugihara, T.J Strathmann, Continuous-flow photocatalytic treatment of pharmaceutical micropollutants: Activity, inhibition, and deactivation of TiO_2 photocatalysts in wastewater effluent, App. Catal. B: Environ. 129 (2013) 1-12. https://doi.org/10.1016/j.apcatb.2012.09.014.

[14] T. Wu, X. Li, D. Zhang, F. Dong, S. Chen, Efficient visible light photocatalytic oxidation of NO with hierarchical nanostructured 3D flower-like $BiOCl_xBr_{1-x}$ solid solutions, J. Alloys Compd. 671 (2016) 318–327. https://doi.org/10.1016/j.jallcom.2016.01.267.

[15] Z. Jia, F. Wang, F. Xin, B. Zhang, Simple Solvothermal Routes to Synthesize 3D $BiOBr_xI_{1-x}$ Microspheres and their visible light induced photocatalytic properties, Ind. Eng. Chem. Res. 50 (2011) 6688–6694. https://doi.org/10.1021/ie102310a.

[16] K. Zhang, C. Liu, F. Huang, C. Zheng, W. Wang, Study of the electronic structure and photocatalytic activity of the BiOCl photocatalyst, Appl. Catal. B: Environ. 68 (2006) 125-129. https://doi.org/10.1016/j.apcatb.2006.08.002.

[17] Preventing occupational exposure to cytotoxic and other hazardous drugs. European Policy Recommendations, European Parliament. https://www.europeanbiosafetynetwork.eu/wp content/uploads/2016/05/Exposure-to CytotoxicDrugs_Recommendation_DINA4_10-03-16.pdf, 2016 (accessed 14 July 2020).

[18] Y. Bai, L. Ye, T. Chen, P. Wang, L. Wang, X. Shi, P.K. Wong, Synthesis of hierarchical bismuth-rich $Bi_4O_5Br_xI_{2-x}$ solid solutions for enhanced photocatalytic activities of CO_2 conversion and Cr(VI) reduction under visible light, Appl. Catal. B Environ. 203 (2017) 633–640. https://doi.org/10.1016/j.apcatb.2016.10.066.

[19] E.M. Siedlecka, A. Ofiarska, A. Fiszka Borzyszkowska, A. Białk-Bielińska, P. Stepnowski, A. Pieczyńska, Cytostatic drug removal using electrochemical oxidation with BDD electrode: Degradation pathway and toxicity, Water Res. 144 (2018) 235-245. https://doi.org/10.1016/j.watres.2018.07.035.

[20] Q. Xiao, L. Ouyang, Photocatalytic activity and hydroxyl radical formation of carbon-doped TiO_2 nanocrystalline: Effect of calcination temperature, Chem. Eng. J. 148 (2009) 248-253. https://doi.org/10.1016/j.cej.2008.08.024.

[21] M. Jia, X. Hu, S. Wang, Y. Huang, L. Song, Photocatalytic properties of hierarchical BiOXs obtained via an ethanol-assisted solvothermal process, J. Environ. Sci. 35 (2015) 172-180. https://doi.org/10.1016/j.jes.2014.09.045.

[22] R. E. Khatib, B. S. Lartiges, A. El Smrani, P. Faure, J. Houhou, J. Ghanbaja, Speciation of Organic Matter and Heavy Metals in Urban Wastewaters from an Emerging Country, Water Air Soil Pollut. 223 (2012) 4695-4708. https://doi.org/10.1007/s11270-012-1226-1

[23] P. Wilczewska, A. Bielicka-Giełdoń, A. Fiszka Borzyszkowska, J. Ryl, E.M. Siedlecka, Photocatalytic activity of solvothermal prepared BiOClBr with imidazolium ionic liquids as a halogen sources in cytostatic drugs removal, J. Photoch. Photobio. A 382 (2019) 111932. https://doi.org/10.1016/j.jphotochem.2019.111932.

[24] A. Latała, S. Jodłowska, F. Pniewski, Culture Collection of Baltic Algae (CCBA) and characteristic of some strains by factorial experimental approach. Algological Stud. 122 (2006) 137-154. https://doi.org/10.1127/1864-1318/2006/0122-0137.

[25] A. Latała, M. Nędzi, P. Stepnowski, Acute toxicity assessment of perfluorinated carboxylic acides towards the Baltic microalgae, Environ. Toxicol. Phar. 28 (2009) 167-171. https://doi.org/10.1016/j.etap.2009.03.010.

[26] International Organization for Standardization (ISO), 2006. Water quality — Marine algal growth inhibition test with *Skeletonema costatum* and *Phaeodactylum tricornutum*. Standard ISO 10253. International Organization for Standardization, Geneva, Switzerland.

[27] OECD, 2011. Test No. 201: Freshwater Alga and Cyanobacteria, Growth Inhibition Test. OECD Guidelines for the Testing of Chemicals, Section 2.

[28] J. Zhang, Q. Han, J. Zhu, X. Wang, A facile and rapid room-temperature route to hierarchical bismuth oxyhalide solid solutions with composition-dependent photocatalytic activity, J. Colloid Interface Sci. 477 (2016) 25-33. https://doi.org/10.1016/j.jcis.2016.05.027.

[29] S. Shewani-Khalil, V. Uvarov, S. Fronton, I. Popov, Y. Sasson, A novel class of heterojunction photocatalysts with highly enhanced visible light photocatalytic performances: $yBiO(Cl_xBr_{1-x})$-(1-y) bismuth oxide hydrate. Appl. Catal. B: Environ. 117-118 (2012) 148-155. https://doi.org/10.1016/j.apcatb.2012.01.011.

[30] A.C. Mera, A. Martinez-de la Cruz, E. Perez-Tijerina, M.F Melendrez, H. Valdes, Nanostructured BiOI for air pollution control: Microwave-assisted synthesis, characterization and photocatalytic activity toward NO transformation under visible light irradiation, Mater. Sci. Semicond. Process. 88 (2018) 20-27. https://doi.org/10.1016/j.mssp.2018.04.045.

[31] A. Bielicka-Giełdoń, P. Wilczewska, A. Malankowska, K. Szczodrowski, J. Ryl, A. Zielińska-Jurek, E. M. Siedlecka, Morphology, surface properties and photocatalytic activity of the bismuth oxyhalides semiconductors prepared by ionic liquid assisted solvothermal method, Sep. Purif. Technol. 217 (2019) 164-173. https://doi.org/10.1016/j.seppur.2019.02.031.

[32] X. Gao, W. Peng, G. Tang, Q. Guo, Y. Luo, Highly efficient and visible-light-driven BiOCl for photocatalytic degradation of carbamazepine, J. Alloys and Compd. 757 (2018) 455-465. https://doi.org/10.1016/j.jallcom.2018.05.081.

[33] Y.L. Qi, Y.F. Zheng, X.C. Song, Synthetic adjustable energy band structure of $BiPO_4$-$BiOCl_xBr_{1-x}$ p-n heterojunctions with excellent photocatalytic activity, J. Taiwan Inst. Chem. E. 77 (2017) 216-226. https://doi.org/10.1039/C9RA01416K.

[34] X. Zhang, L.-W. Wang, C.-Y. Wang, W.-K. Wang, Y.-L. Chen, Y.-X. Huang, W.-W. Li, Y.-J. Feng, H-Q. Yu, Synthesis of $BiOCl_xBr_{1-x}$ Nanoplate Solid Solutions as a Robust Photocatalyst with Tunable Band Structure, Chem. Eur. J. 21 (2015) 11872-11877. https://doi.org/10.1002/chem.201501427.

[35] D. Zhang, H. Liu, C. Su, H. Li, Y. Geng, Combustion synthesis of highly efficient Bi/BiOBr visible light photocatalyst with synergetic effects of oxygen vacancies and surface plasma resonance, Sep. Purif. Technol. 218 (2019) 1-7. https://doi.org/10.1016/j.seppur.2019.02.037.

[36] H.H.-H. Lin, A.Y.-C. Lin, Photocatalytic oxidation of 5-fluorouracil and cyclophosphamide via UV/TiO$_2$ in an aqueous environment, Water Res. 48 (2014) 559-568. https://doi.org/10.1016/j.watres.2013.10.011.

[37] J. Li, S. Sun, R. Chen, T. Zhang, B. Ren, D.D Dionysiou, Z. Wu, X. Liu, M. Ye, Adsorption behavior and mechanism of ibuprofen onto BiOCl microspheres with exposed {001} facets, Environ. Sci. Pollut. Res. 24 (2017) 9556-9565. https://doi.org/10.1007/s11356-017-8564-x578 (2017) 257-267. https://doi.org/10.1016/j.scitotenv.2016.08.208.

[38] A. Koltsakidou, M. Antonopoulou, E. Evgenidou, I. Konstantinou, A.E. Giannakas, M. Papadaki, D. Bikiaris, D.A. Lambropoulou, Photocatatytical removal of fluorouracil using TiO$_2$-P25 and N/S doped TiO$_2$ catalysts: A kinetic and mechanistic study, Sci. Total Environ.

[39] B.D Witte, H.V. Langenhove, K. Demeestere, K. Saerens, P.D. Wispelaere, J. Dewulf, Ciprofloxacin ozonation in hospital wastewater treatment plant effluent: Effect of pH and H$_2$O$_2$, Chemosphere 78 (2010) 142-147. https://doi.org/10.1016/j.chemosphere.2009.12.026.

[40] K.M.S. Hansen, A. Spiliotopoulou, R.K. Chhetri, M.E. Casas, K. Bester, H.R. Andersen, Ozonation for source treatment of pharmaceuticals in hospital wastewater– ozone lifetime and required ozone dose, Chem. Eng. J. 290 (2016) 507-514. https://doi.org/10.1016/j.cej.2016.01.027.

[41] A. Amouei, H. Asgharnia, H. Fallah, H. Faraji, R. Barari, D. Naghipour, Characteristics of Effluent Wastewater in Hospitals of Babol University of Medical Sciences, Health Scope 4 (2015) 1-4. https://doi.org/10.17795/jhealthscope-23222.

[42] X. Zhang, P. Yang, B. Yang, Y. Bai, W. Liu, K. Zhang, Synthesis of the composite catalyst Bi4O5Br2/BiOBr for the improved photocatalytic degradation of oilfield produced wastewater, J. Mater. Sci.: Mater. Electron. 30 (2019) 17276-17287. doi:10.1007/s10854-019-02074-6

[43] X. Gao, X. Zhang, Y. Wang, S. Peng, B. Yue, C. Fan, Rapid synthesis of hierarchcial BiOCl microspheres for efficient photocatalytic degradation of carbamazepine under simulated solar irradiation, Chem. Eng. 263 (2015) 419-426. doi:10.1016/j.cej.2014.10.110

[44] D. Mao, A. Yu, S. Ding, F. Wang, S. Yang, C. Sun, H. He, Y. Liu, K. Yu, One-pot synthesis of BiOCl half-shells using microemulsion droplets as templates with highly photocatalytic performance for degradation of ciprofloxacin, Appl. Surf. Sci. 389 (2016) 742-750. doi:10.1016/j.apsusc.2016.07.178

[45] E. Kudlek, M. Dudziak, J. Bohdziewicz, Influence of Inorganic Ions and Organic Substances on the Degradation of Pharmaceutical Compound in Water Matrix, Water 8 (2016) 532-550. https://doi.org/10.3390/w8110532.

[46] Ch. Guillard, E. Puzenat, H. Lachheb, A. Houas, J.-M. Herrmann, Why inorganic salts decrease the TiO_2 photocatalytic efficiency, Int. J. Photoenergy 7 (2005) 9-19. https://doi.org/10.1155/S1110662X05000012.

[47] K.-H. Wang, Y.-H. Hsieh, Ch.-H. Wu, Ch.-Y. Chang, The pH and anion effects on the heterogeneous photocatalytic degradation of o-methylbenzoic acid in TiO_2 aqueous suspension, Chemosphere 40 (2000) 389-394. https://doi.org/10.1016/S0045-6535(99)00252-0.

[48] B.G. Ershov, P.A. Morozov, A.V. Gordeeev, Effect of silver and copper ions on the decomposition of ozone in water, Russ. J. Phys. Chem. A 86 (2012) 1795-1799. https://doi.org/10.1134/S0036024412120072.

[49] M. Dhananjeyan, R. Annapoorani, R. Renganathan, A comparative study on the TiO_2 mediated photo-oxidation of uracil, thymine and 6-methyluracil, J. Photoch. Photobio. A 109 (1997) 147–153. https://doi.org/10.1016/S1010-6030(97)00119-6.

[50] W.J. Szczepek, B. Kosmacińska, A. Bielejewska, W. Łuniewski, M. Skarżyński, D. Rozmarynowska, Identification of imatinib mesylate degradation products obtained under stress conditions, J. Pharm. Biomed. 43 (2007) 1682-1691. https://doi.org/10.1016/j.jpba.2006.12.033.

Supplementary material

Application of BiOCl$_n$Br$_m$ photocatalyst to cytostatic drugs removal from water; mechanism and toxicity assessment

Patrycja Wilczewska[1], Andrea Elisabeth Natasha Ona[2], Aleksandra Bielicka Giełdoń[1], Anna Malankowska[1], Karol Tabaka[1], Jacek Ryl[3], Filip Pniewski[4], Ewa Maria Siedlecka[1]*

[1]Faculty of Chemistry, University of Gdansk, Wita Stwosza 63, 80-308 Gdansk, Poland

[2]Escurla Politécnica Nacional, Departamento de Ingeniería Civil y Ambiental, Centro de Investigación y Control Ambiental, Ladrón de Guevara E11-253, Quito, Ecuador, P.O. Box 17-01-2759.

[3]Faculty of Chemistry, Gdansk University of Technology, Narutowicza 11/12, 80-233 Gdansk, Poland

[4]University of Gdańsk, Institute of Oceanography, Laboratory of Marine Plant Ecophysiology, al. Marszałka Piłsudskiego 46, 81-378 Gdynia, Poland

*Coresponding author:

Ewa Siedlecka e-mail: ewa.siedlecka@ug.edu.pl; phone: +48 58 5325228

Experiments with cytostatic drugs

Works with cytostatic drugs were carried out following the recommendation of the European Commission: "Preventing occupational exposure to cytotoxic and other hazardous drugs [17].

Everyone working with cytostatic drugs has been trained in the proper selection and use of personal protective equipment. All work-related to cytostatic drugs was performed in a specially designated, well-ventilated laboratory. Personnel exposed to cytostatic drugs were equipped with protective gloves, protective clothing, goggles, face protection, and shoe covers. To enable quick response in emergencies, the laboratory where cytostatic drugs were tested was equipped with a spill kit. All materials - personal protective equipment, laboratory equipment, materials used to clean the work surface, were single-use and were placed in hazardous waste containers.
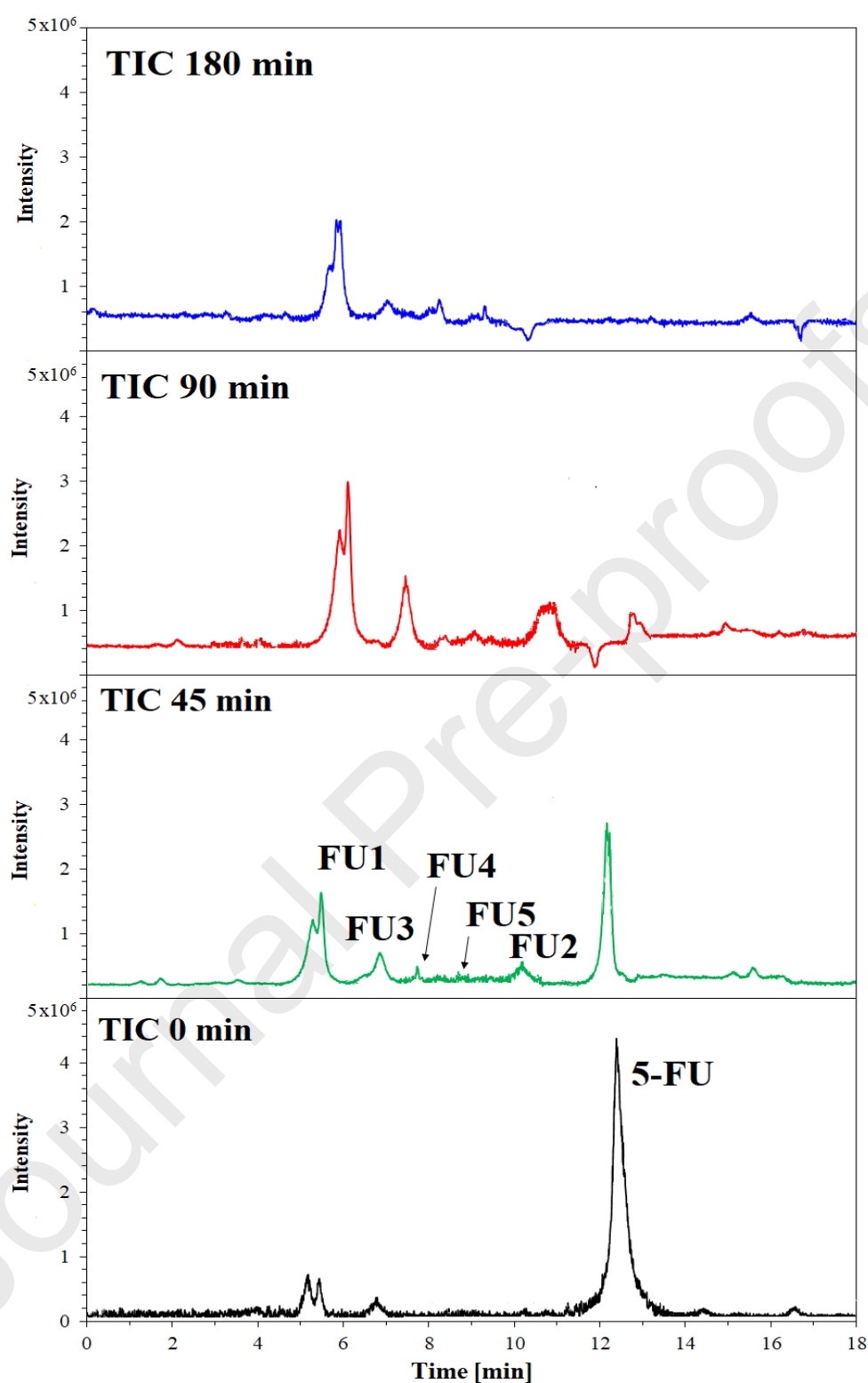
Figure S1. Total ion current (TIC) chromatogram in negative mode of effluents after different times illumination by sunlight of 5-FU solution.
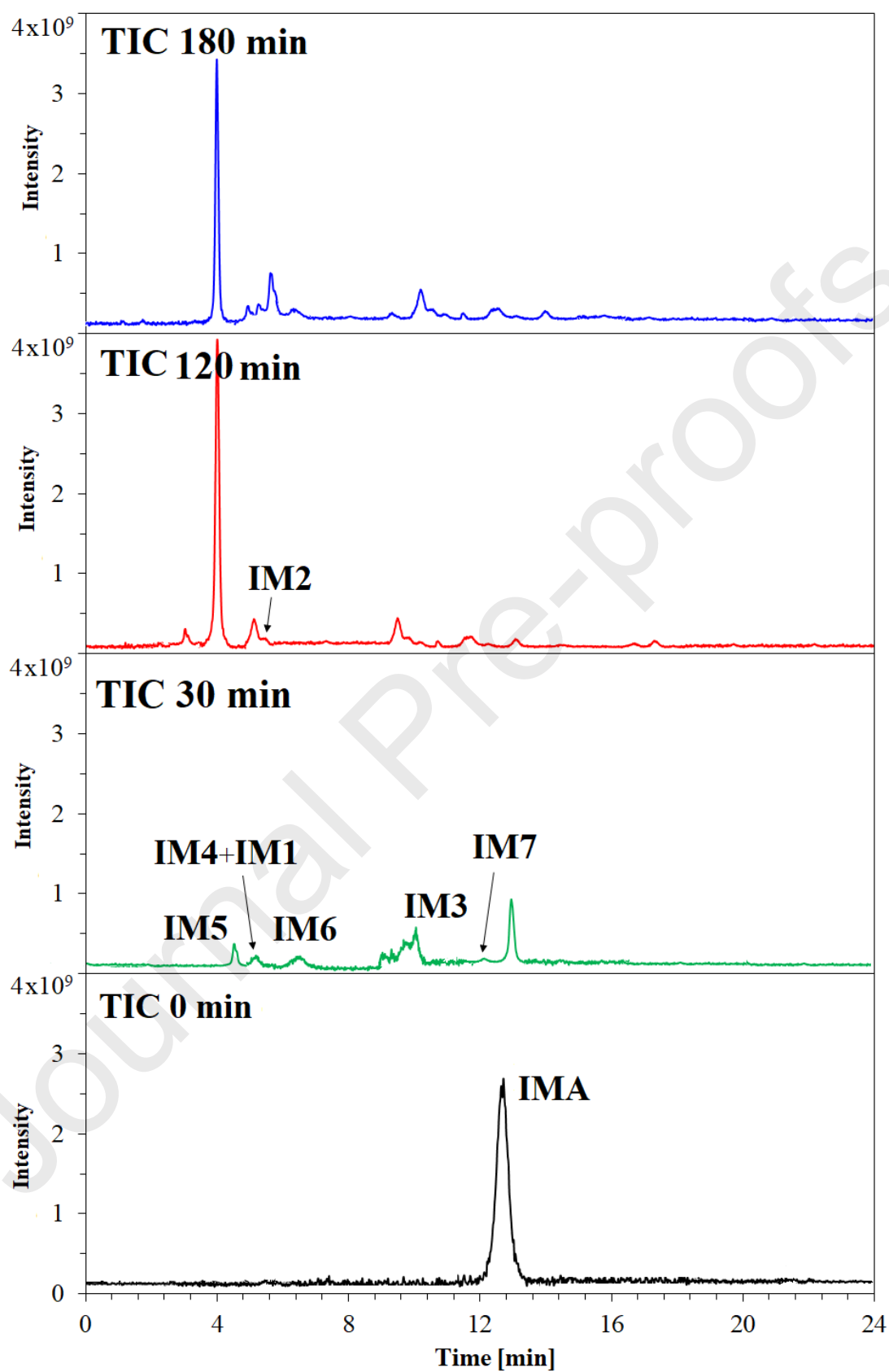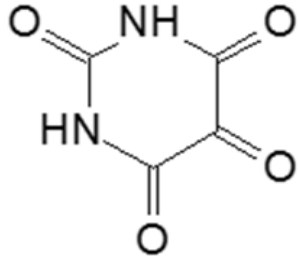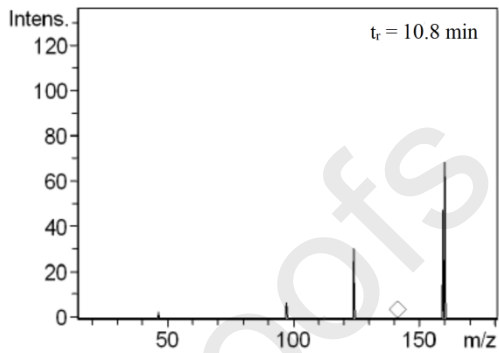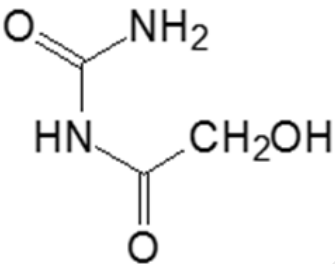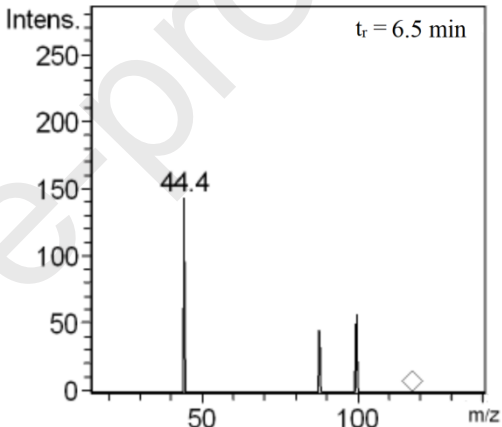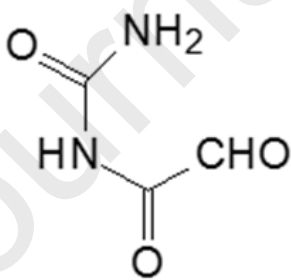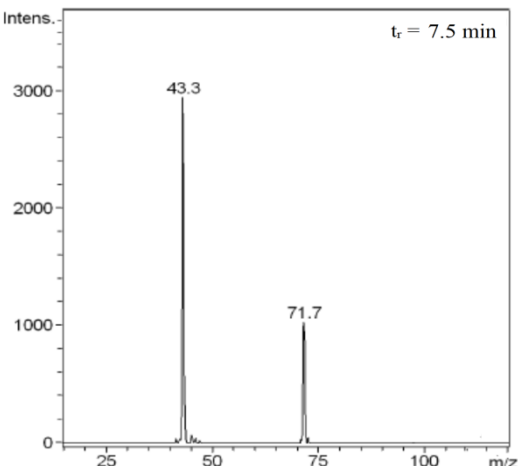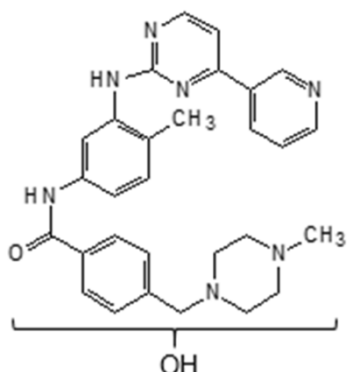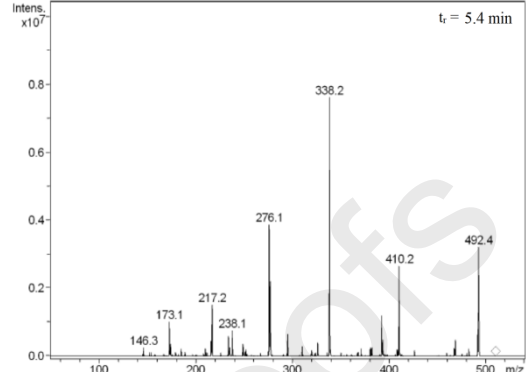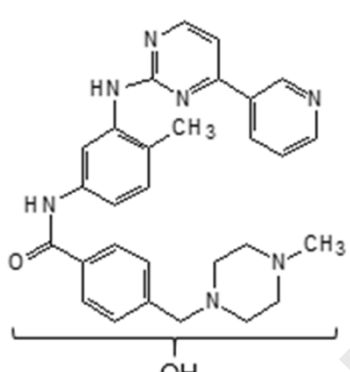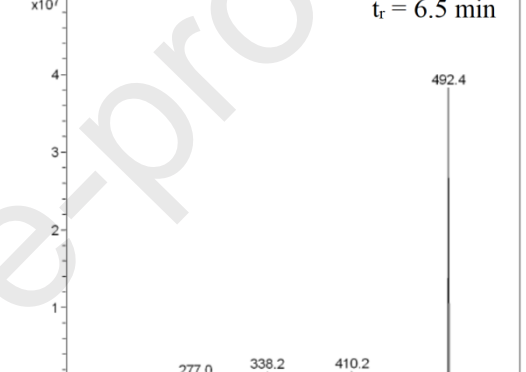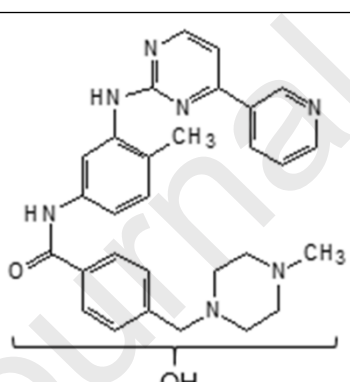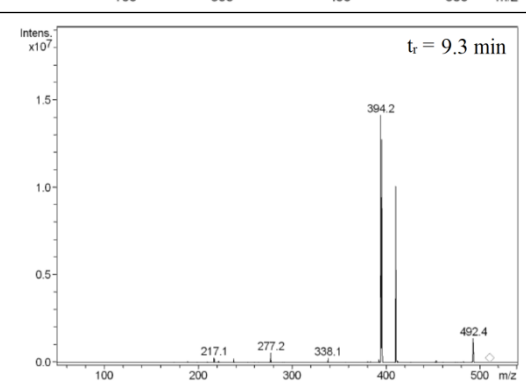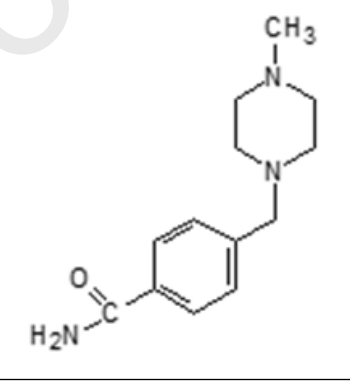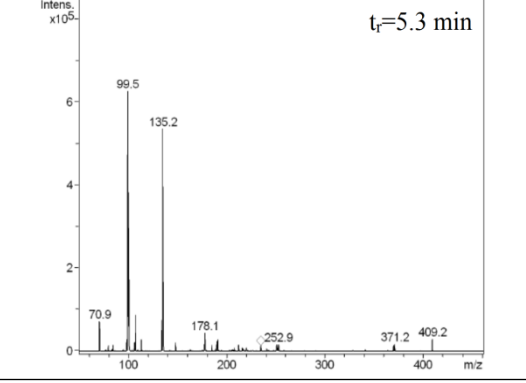
Figure S2. Total ion current (TIC) chromatogram in positive mode of effluents after different times illumination by sunlight of IMA solution

Table S1. Selected intermediates found after photocatalysis of 5-FU over BiOCl1.3Br0.7 under solar light irradiation

Label	Intermediate structure	[M-H]⁻ m/z$_{(cal)}$	Fragmentation spectra
FU1	unknown	155	-
FU2		141.0 142.07	
FU3		117.0 118.08	
FU4		115.0 116.07	

m/z$_{(cal)}$ – calculated from chemical formula m/z values

Table S2. Selected intermediates found after photocatalysis of IMA over BiOCl1.3Br0.7 under solar light irradiation

Label	Intermediate structure	$[M+H]^+$ $m/z_{(cal)}$	Fragmentation spectra
IM1		510.5 509.60	
IM2		510.5 509.60	
IM3		510.5 509.60	
IM4		234.6 233.6	

| IM7 | | 277.0
276.32 | |
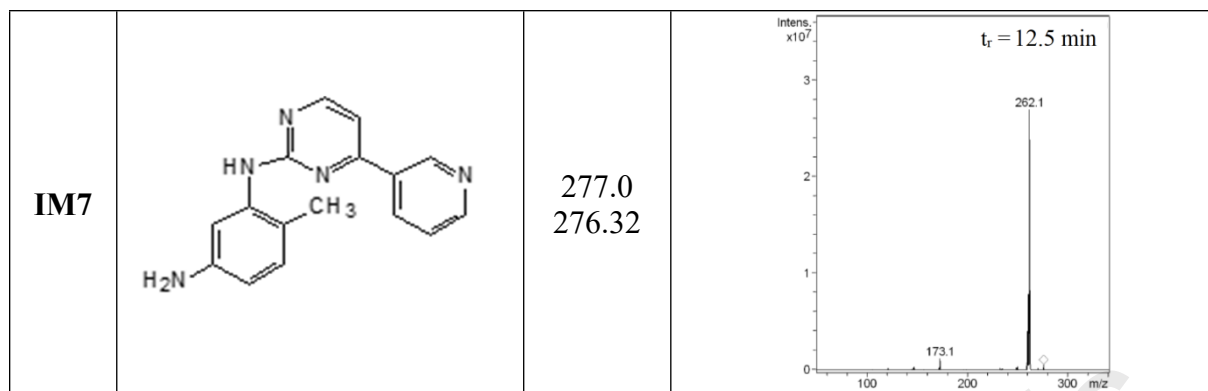
m/z$_{(cal)}$ – calculated from chemical formula m/z values

Patrycja Wilczewska : investigation, validation, visualisation,

Andrea Elisabeth Natasha Ona: investigation,

Aleksandra Bielicka Giełdoń: data curation, writing - Editing, resources ,

Anna Malankowska: investigation,

Karol Tabaka: visualisation,

Jacek Ryl: investigation,

Filip Pniewski: investigation, draft part preparation,

Ewa Maria Siedlecka: conceptualization, methodology, Writing - Original Draft preparation, funding acquisition.

- BiOCl1.3Br0.7 effectively removed IMA and 5-FU singly and in their mixture
- Inorganic anions has significant effect on IMA adsorption at BiOCl1.3Br0.7
- IMA and inorganic anions significantly inhibited the 5-FU removal
- Holes mainly participated in drugs degradation, but not its mineralization
- Toxicity decreased after photodegradation of IMA and 5-FU singly and in mixture